FINAL REPORT

LUNAR MASS SPECTROMETER
TEST PROGRAM

By F. L. Torney and J. R. Dobrott

FINAL REPORT

LUNAR MASS SPECTROMETER
TEST PROGRAM

By F. L. Torney and J. R. Dobrott

Prepared Under Contract No. NASw-2114

by

National Research Corporation
(A Subsidiary of Cabot Corporation)
Cambridge, Massachusetts

for

NATIONAL AERONAUTICS AND SPACE ADMINISTRATION

TABLE OF CONTENTS

Page

LIST OF FIGURES

LUNAR MASS SPECTROMETER TEST PROGRAM

By F. L. Torney and J. R. Dobrott
National Research Corporation

SUMMARY

This report describes the procedures used, and the results obtained in a test program conducted to demonstrate the performance of a candidate lunar mass spectrometer. The instrument is designed to sample and measure gases believed to exist in the lunar atmosphere at the surface. The subject instrument consists of a cold cathode ion source, a small quadrupole mass analyzer and an off axis electron multiplier ion counting detector. The major program emphasis was placed on demonstrating instrument resolution, sensitivity and S/N ratio over the mass range 0-150 amu and over a partial pressure range from 10^{-9} Torr to $< 10^{-13}$ Torr.

The subject analyzer was also prepared for extended testing, in conjunction with two other candidate instruments, in a large molecular beam vacuum facility. Although this portion of the test program was not conducted, the minimum detectable partial pressure for neon, argon, krypton and xenon was successfully determined for the spectrometer using isotopes of these gases. With the exception of neon, the minimum detectable partial pressure is approximately 4×10^{-14} Torr for the above gases.

INTRODUCTION

The measurement and analysis of the very tenuous lunar atmosphere requires a high sensitivity, low power, rugged mass spectrometer with a relatively wide mass range (0-150 amu) and with an adequate resolving power (> 100). Additionally, the spectrometer must be free of internal gas sources which could produce interfering spectral peaks.

Certain candidate instruments have been proposed for this type of measurement. Accordingly, a test program was planned to evaluate these instruments simultaneously in a large molecular beam facility. Prior to the initiation of these tests, each instrument was required to undergo preliminary performance tests to demonstrate its capability of meeting specified design goals. In addition, each instrument was to be prepared for integration with the others in a standard test fixture so that all operating and test conditions would be similar.

This report describes the preparation and performance testing of one of these candidate instruments; namely the cold cathode ion source/quadrupole (CCIS/Quad) mass spectrometer. In lieu of the comparison tests originally planned, but not conducted, additional ultra-high vacuum (UHV) tests were made at the contractor's facility. The purpose of these tests was to determine and demonstrate the minimum detectable partial pressure of the spectrometer for the inert gases (except helium). The results of these tests are also described herein.

2

LIST OF SYMBOLS AND ABBREVIATIONS

B	magnetic field (gauss)
CCIS	cold cathode ion source
CCIS/Quad	cold cathode ion source/quadrupole
cpm	counts per minute
cps	counts per second
Disc.	discriminator setting (volts)
Δm	peak width, at 5% of height (amu)
I_c	collector current (amperes)
I_K	CCIS first cathode current (amperes)
K_1	CCIS first cathode
K_2	CCIS second (exit) cathode
m	mass (atomic mass units)
$m/\Delta m$	resolving power
MBAG	Modulated Bayard-Alpert Gauge
P	pressure (Torr)
Res.	resolution setting (arbitrary units)
r_o	radius of circle inscribed within quadrupole rod structure (meter)

S_d	detector sensitivity (pulses per second/Torr)
S/N	signal-to-noise ratio
UHV	ultrahigh vacuum (pressure $< 10^{-9}$ Torr)
V_A	anode potential (volts)
V_M	multiplier voltage (volts)
V_D	deflector plate potential (volts)
V_R	retarding potential (volts)

4

LUNAR ATMOSPHERE MASS SPECTROMETER TEST PROGRAM

Description of Program Scope
and Objectives

Previous Related Developments. - Under a previous NASA
sponsored program (ref. 1), a prototype lunar mass spectro-
meter (less electronics) was designed and developed. This
instrument featured a cold cathode ion source[*], a quadrupole
mass analyzer, and an electron multiplier ion counting de-
tector. The instrument was designed to measure gaseous species
in the 1-150 amu range, with a resolving power $(m/\Delta m)$ of 100
or greater and with a minimum power and weight budget (< 10 lbs.,
10 watts). The minimum detectable partial pressure was estimated
to be < 1×10^{-13} Torr (nitrogen @ 300°K), based on preliminary
test results.

With certain modifications, to be detailed herein, the
prototype instrument was prepared for a two-phase test program,
to demonstrate the performance of the instrument under simulated
lunar conditions.

Test Program Purpose, Scope and Objectives. - As set
forth in the original contract STATEMENT OF WORK, the purpose
and scope of the test program is as follows:

> The purpose of the test program is to demonstrate
> the characteristics and performance of three different

---

[*]See refs. 2-5 for additional background material on cold
cathode ion source mass spectrometers.

5

mass spectrometers* which could be used to measure the composition of the lunar atmosphere. The three instruments are a magnetic sector field mass spectrometer, a cold cathode ion source quadrupole, and a hot filament source quadrupole. The testing program will consist of (a) initial "in house" tests to be performed separately by each contractor, and (b) comparison tests* of these instruments under the high vacuum and more accurately controlled environment of a Molecular Beam Facility.

The objectives of the test program are as follows:

a) To determine the capability of each instrument to respond to partial pressures of various gases believed to exist at the lunar surface.

b) To determine the comparative performance of the instruments.

The basic design goals for the mass spectrometer may be summarized as follows:

a) Mass Range: 1 to 150 amu (5-11 amu optional).

b) Dynamic Range: 5 orders of magnitude

c) Resolution: at mass 135 less than 1% contribution from either of the adjacent peaks (Xe^{134} or Xe^{136}). Less than a 50% valley between Xe^{131} and Xe^{132}. Less than 1 part in 300 of the mass 40 peak (Ar^{40}) at mass 39.

---

*This report details the test results obtained on only one of the three spectrometers, namely, the cold cathode ion source/ quadrupole instrument. The comparison tests of the three candidate instruments in a molecular beam facility were not performed.

d) Minimum Detectable "Partial Pressure": 10^{-14} Torr equivalent N_2.

e) Output Response Characteristics: Output for a given gas pressure input is to be unique and repeatable.

f) Sweep Time: Less than 1 hour for the entire mass range.

g) High Pressure Limit: Survival of 10^{-5} Torr pressure during instrument operation.

h) Weight, Power, and Size: Compatible with lunar mission constraints.

<u>In House Test Procedures</u>. - The following test procedures describe the general tests which were conducted by the contractor at his facility. Additional tests were performed in connection with the general evaluation of the instrument's performance.

a) Mass Range: Demonstrate the coverage of the mass range from 1 to 150 amu by taking a spectrum of a gas mixture containing both light, medium and heavy gases such as helium, neon, nitrogen, argon, carbon dioxide, krypton and xenon.

b) Dynamic Range: Demonstrate the dynamic range by taking the spectrum of a mixture of gases in which there are several orders of magnitude difference between the various constituents. An electron multiplier and counting circuits should be used to develop the output. Conceivably, the same gas mixture can be used for both the mass range and dynamic range tests.

c) Resolution: Demonstrate the resolution as
    defined in the design goals by taking the
    spectra of argon and xenon and specify the
    sensitivity of the instrument corresponding
    to the resolution spectra.

d) Sweep Time: Demonstrate the sweep time,
    not to exceed 1 hour, required to cover the
    mass range from 1 to 150 amu. This test
    can be combined with the mass range test.
    The test shall be carried out with argon
    gas at a pressure of 10^{-9} Torr in the
    source. The sweep time, the source pressure
    and the number of counts for the mass 40
    peak will be recorded.

e) Weight, Power and Size: Prepare estimates
    of the weight, power and size of each
    instrument based on measured parameters
    obtained during the in house tests.

In lieu of the molecular beam facility tests originally
scheduled, additional UHV tests were conducted by the contractor
as will be described separately in a later section of this re-
port.

Preparation for Test Program

Prior to conducting the in house tests described above,
certain preliminary work was performed in order to prepare
the CCIS/Quad sensor/analyzer and other ancillary equipment
for these tests. Briefly stated, this work involved the
following:

8

1. Baseline experimentation prior to modification of the CCIS/Quad analyzer.

2. Modification of the laboratory type quadrupole drive electronics for long cable operation.

3. Modification and preparation of the CCIS/Quad analyzer.

4. Modification and preparation of the laboratory UHV system for the in house tests.

5. Design and fabrication of special bakeout heaters and adapter flanges to be used during the molecular beam facility tests.

Baseline Experimentation. - Before modifications were made to the sensor/analyzer developed under the previous contract (ref. 1), dc spectra of the UHV residual gases were taken to determine approximate values of sensitivity, resolution and photon background noise of the instrument. Ion counting techniques were also employed to determine ion and photon pulse height distributions and multiplier thermionic dark current noise. A survey was also made of the magnetic field surrounding the unshielded ion source magnet. If was found that for distances between 7 and 30 cm from the magnet center, the magnetic field along a line perpendicular to the magnet axis approximates the familiar $1/d^3$ dipole field relation. A field of approximately 0.6 gauss was measured 30 cm from the magnet center.

In general the results of these brief experiments confirmed data previously reported in ref. 1.

<u>Modification of Quadrupole Electronics</u>. - The comparison
tests originally scheduled to be conducted in a large mole-
cular beam vacuum facility necessitated the CCIS/Quad operating
electronics to be located outside the vacuum system. Approxi-
mately fifteen feet of rf cable would be required to locate
the quadrupole drive electronics at a convenient point outside
the facility. The increased capacity associated with long
cables reduces the rf operating frequency of the quadrupole
electronics which in turn, adversely effects sensitivity and/
or resolution of the instrument.

Previous work (ref. 1) established that the optimum
operating frequencies for the CCIS/Quad were 6 mHz and 4 mHz
on the 0-50 amu and 10-150 amu ranges, respectively. The out-
put frequency of the quadrupole electronics is determined by
the L-C tank circuit comprising the inductance of the output
transformer, the capacitance of the quadrupole rod assembly,
and connecting cables. To compensate for the increased
capacitance (121 pf each cable), the output inductance of
the rf transformers was decreased.

It was found that the desired 4 mHz rf frequency could
readily be obtained on the medium range by direct substitution
of a standard low range transformer for the medium range
transformer normally used. The 6 mHz rf frequency was then
obtained by decreasing the number of turns on a second low
range transformer from 17 to 11 turns. Three turns were re-
moved from each end to maintain output symmetry. The measured
frequencies obtained by these modifications were 3.98 mHz
(medium range) and 5.8 mHz (low range). These frequencies re-
mained unchanged throughout subsequent tests.

10

In addition to the above modifications, other adjustments were made to the quadrupole drive electronics to obtain more uniform sensitivity and resolution across the overall mass range. These adjustments are detailed in the APPENDIX section of this report.

After modifying the quadrupole electronics for the longer cables, baseline performance of the instrument was again briefly evaluated. No problems were encountered.

CCIS/Quad Preparation. - Once the operating electronics was modified, the CCIS/Quad sensor/analyzer was modified and prepared for the test program as described below.

In order to prevent splitting of the mass peaks reported by Arnold (ref. 6), a means was provided to accurately maintain alignment of the quadrupole entrance aperture and the rod assembly axis, shown in Figure 1. This was accomplished by moving the first ceramic insulator flush with the end of the rod assembly and fabricating a new cathode pole piece with a .010" lip extending between the insulator and the CCIS housing. The lip was machined to provide a press fit between the insulator and pole piece, thus rigidly maintaining the required alignment. The new pole piece also effectively isolates the ion source from the analyzer/detector section and therefore reduces background gas within the ion source, as will be discussed shortly.

To further minimize ion source outgassing, the CCIS cathode plates K_1 and K_2, the anode cylinder, and the new pole piece were vacuum degassed at 500°C by rf induction heating in vacuum (10^{-6} Torr) for approximately 2½ hours. Additionally, the entire CCIS housing assembly was also rf induction heated in vacuum to reduce outgassing, particularly hydrogen. The cathode
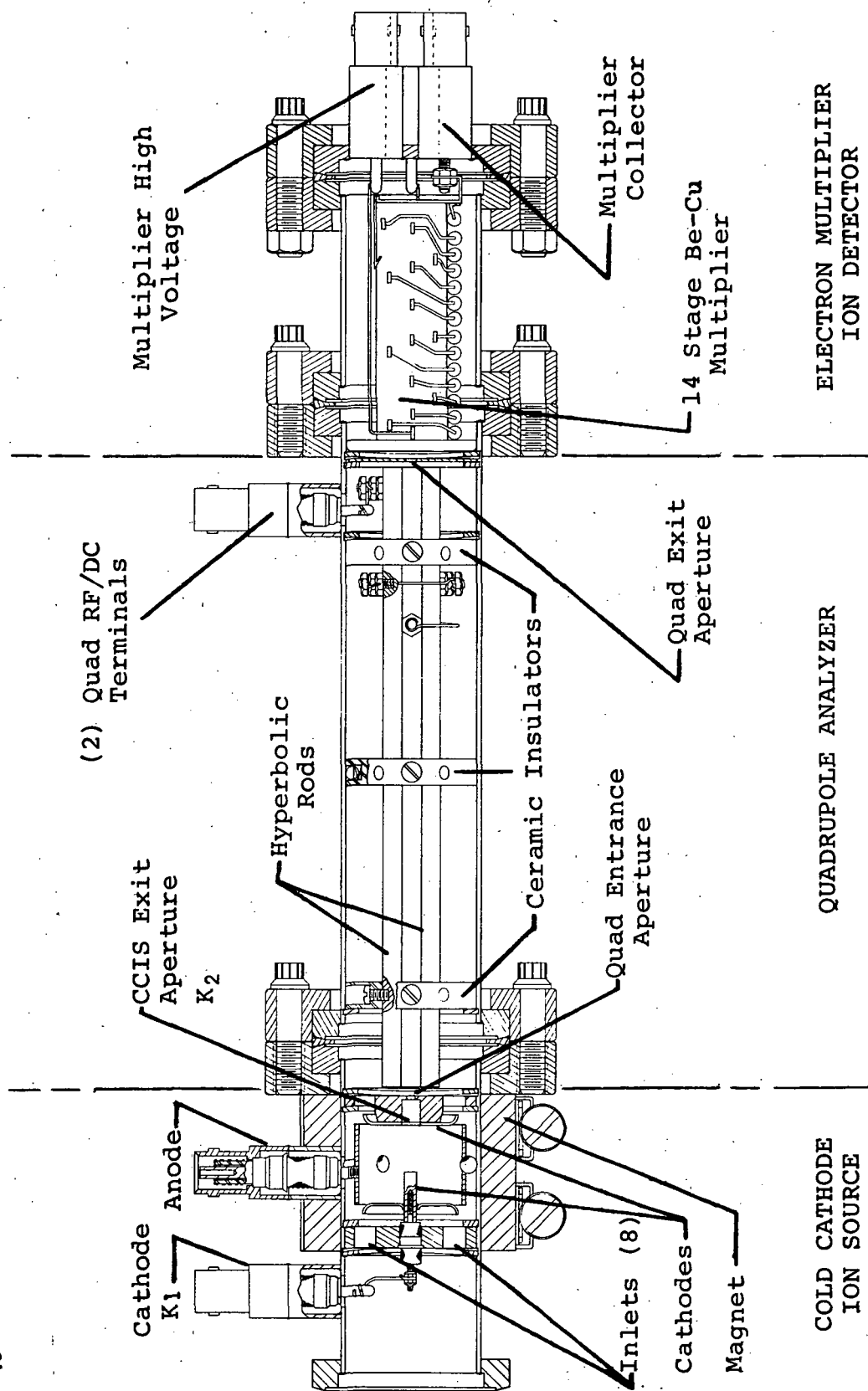
FIG. 1 – COLD CATHODE ION SOURCE/QUADRUPOLE (SECTIONAL VIEW)

12

plates and the anode cylinder were polished and ultrasonically cleaned prior to vacuum firing. Similar procedures were followed by NRC during the manufacture of the ALSEP cold cathode ion gauges. Other salutary effects resulting from this procedure, such as improved starting and reduced field emission, were demonstrated by the ALSEP gauge.

A pump-out port was welded to the quadrupole analyzer housing to provide an egress for outgassing of the internal surfaces of the quadrupole-multiplier structure. This port, together with the modified pole piece (K_2), prevents large fluxes of background gas from entering the ion source. Since the pump out port conductance is much larger than the conductance of the exit aperture between the quadrupole and ion source housings, the partial pressure of background gases in the ion source is greatly reduced. A detailed quantitative analysis of this subject appears in the APPENDIX section of this report.

For an actual lunar surface experiment, this port would be directed upward toward free space and would be oriented to prevent solar radiation from entering. For the proposed molecular beam facility test, the port would face a liquid helium wall, thus simulating (as nearly as possible) the environment of a lunar mission.

The final modifications made to the CCIS/Quad involved the choice and mounting of a suitable electron multiplier. The multiplier previously used was a commercially available,[†] 14 stage, "box and grid" type. It was proposed to investigate a smaller, flight-type multiplier[*]. Although the gain for

---

†Made by Electronics Associates, Inc., Palo Alto, California.

*Model MM-2 focused mesh multiplier. Made by Johnston Laboratories, Cockeysville, Maryland.

latter is modest (10^6), the dark current (field emission, leakage and thermionic emission) are specified to be < 1 x 10^{-13} amperes at a gain of 10^6 (for 600 eV electrons). The noise is therefore < 1 electron/sec equivalent at the first dynode.

The new focused-mesh multiplier was compared with the box and grid type. Both multipliers were initially mounted on axis so that ion and photon pulse height distributions could be observed for each multiplier. Figure 2 summarizes the results of this comparison. Although the ionic masses are different, and slight differences in pressure existed in the system during measurement, the influence of these variables on the ion and photon integral pulse height distributions would be small. A pronounced difference is observed in the integral pulse height distribution for photons. A broad photon distribution exists for the small flight type multiplier, while a very narrow photon distribution is observed for the laboratory type multiplier.* It is obvious that the most favorable S/N ratio can be obtained from the laboratory type multiplier by adjusting the discriminator to reject the photon background. For this reason, the laboratory multiplier was chosen for use in the test program.

It should be noted that it is presently impossible to predict the photon pulse height distribution characteristics of either multiplier because no information exists on the energy (wavelength) distributions of photons emanating from

---

*This multiplier has been rejuvenated by an oxygenation process devised by NRC. The flight multiplier was not processed in a like manner.
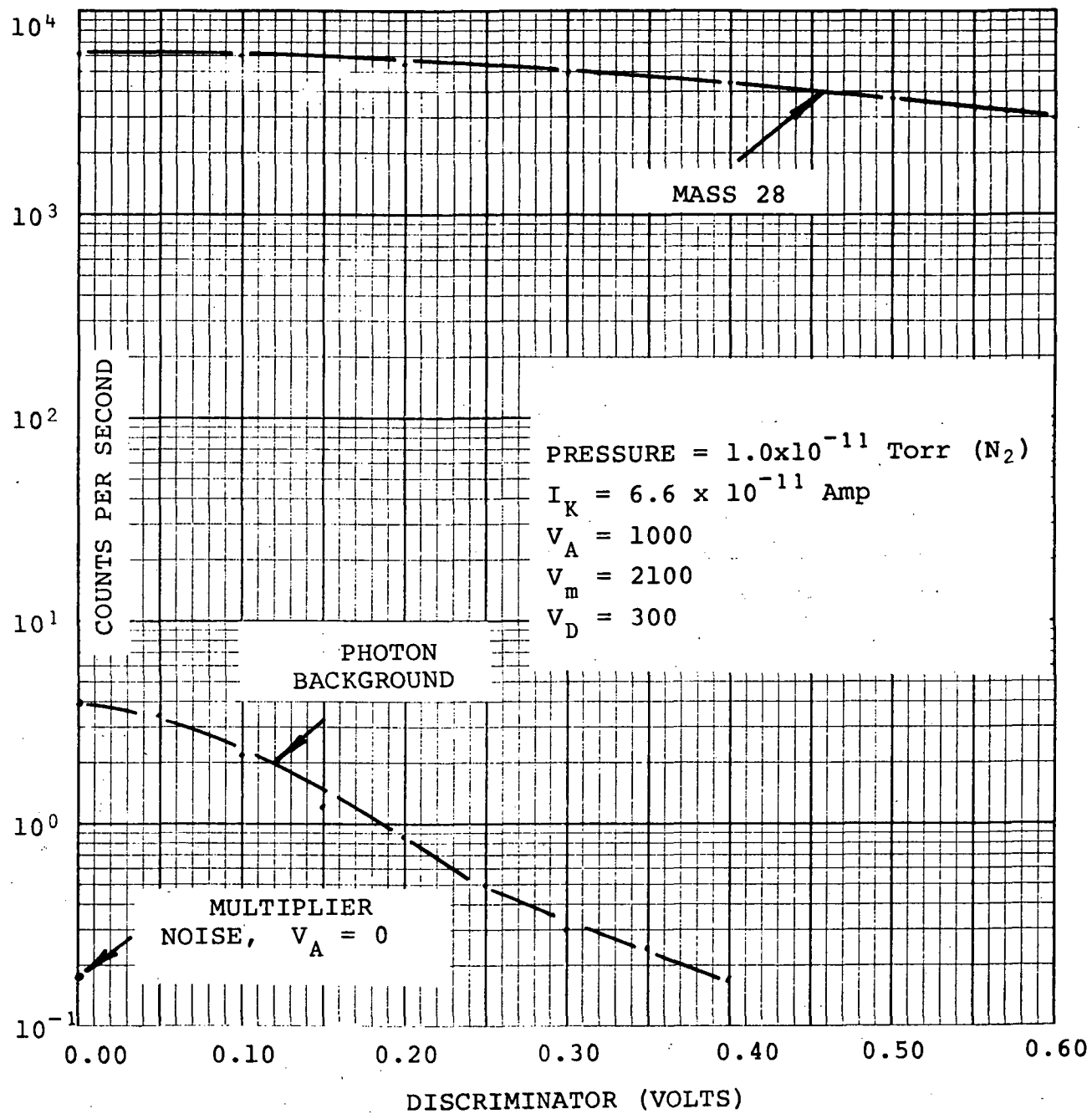
Figure 3. - Integral Pulse Height Distribution. Lab Type Electron Multiplier Off-Axis With Deflector Plates.

18
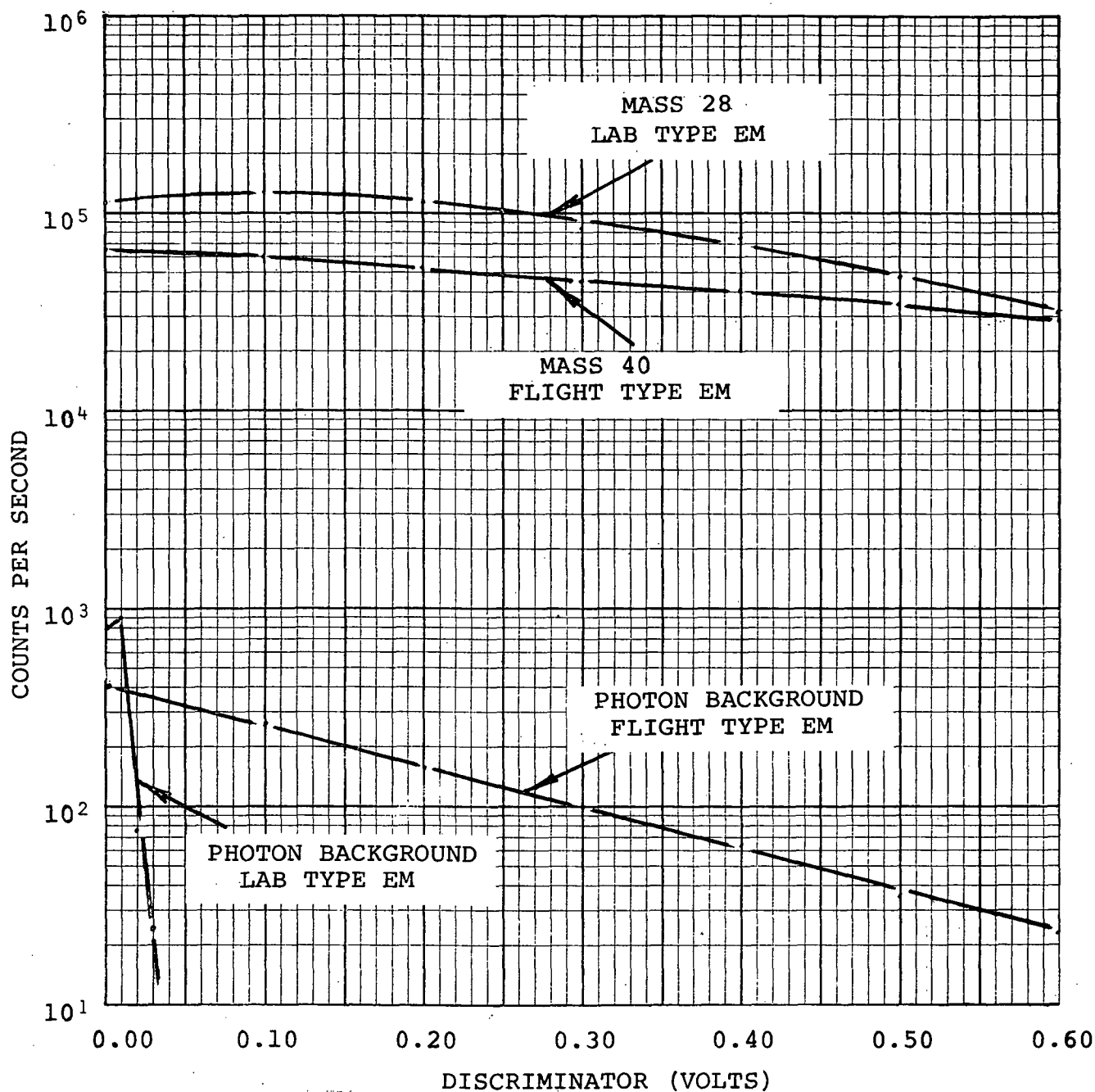
MULTIPLIER	P(TORR N_2)	I_K (AMP)	V_A (VOLTS)	V_m (VOLTS)	G_m
LAB TYPE	1.5×10^{-9}	1.2×10^{-9}	1000	2500	1.73×10^6
FLIGHT TYPE	6.0×10^{-10}	2.15×10^{-10}	1000	2800	1.4×10^6

Figure 2. - Integral Pulse Height Distribution Comparison.

Page Intentionally Left Blank

Page Intentionally Left Blank

this work, the vacuum system was also overhauled as will be briefly described next.

Vacuum System Preparation. - Before any of the experimentation described above was performed, the UHV portion of the test vacuum system was arranged in accordance with the schematic diagram of Figure 4. This diagram shows only that portion of the entire vacuum system which is baked and which later achieves UHV pressures. The UHV valve shown in the figure leads to a lower manifold (not baked) and an ion pump which evacuates the UHV section during bake-out. Additional valves are provided in the lower manifold for admitting test gases, roughing down the system from atmospheric pressure, and for isolating the lower ion pump during air release.

Figure 5 is a photograph of the UHV system with the CCIS/Quad under test. The operating electronics is at the far left. The counting electronics is not shown.

Prior to final assembly, both the upper and lower manifold ion pumps were chemical cleaned using a hot* mixture of:

> 1 part   HCl
> 3 parts HNO_3
> 2 parts HF
> 72 parts H_2O

The above solution was left in the pumps for 1 or 2 minutes and quickly poured off. The pumps were immediately rinsed in cold tap water for one hour and then rinsed again with distilled water. The pumps were then oven baked at 150°C for 2 hours to dry out the residual water.

---

*EXTREME CAUTION must be exercised in heating and handling this solution since it is very corrosive.

Figure 4. - UHV System for Lunar MS Test
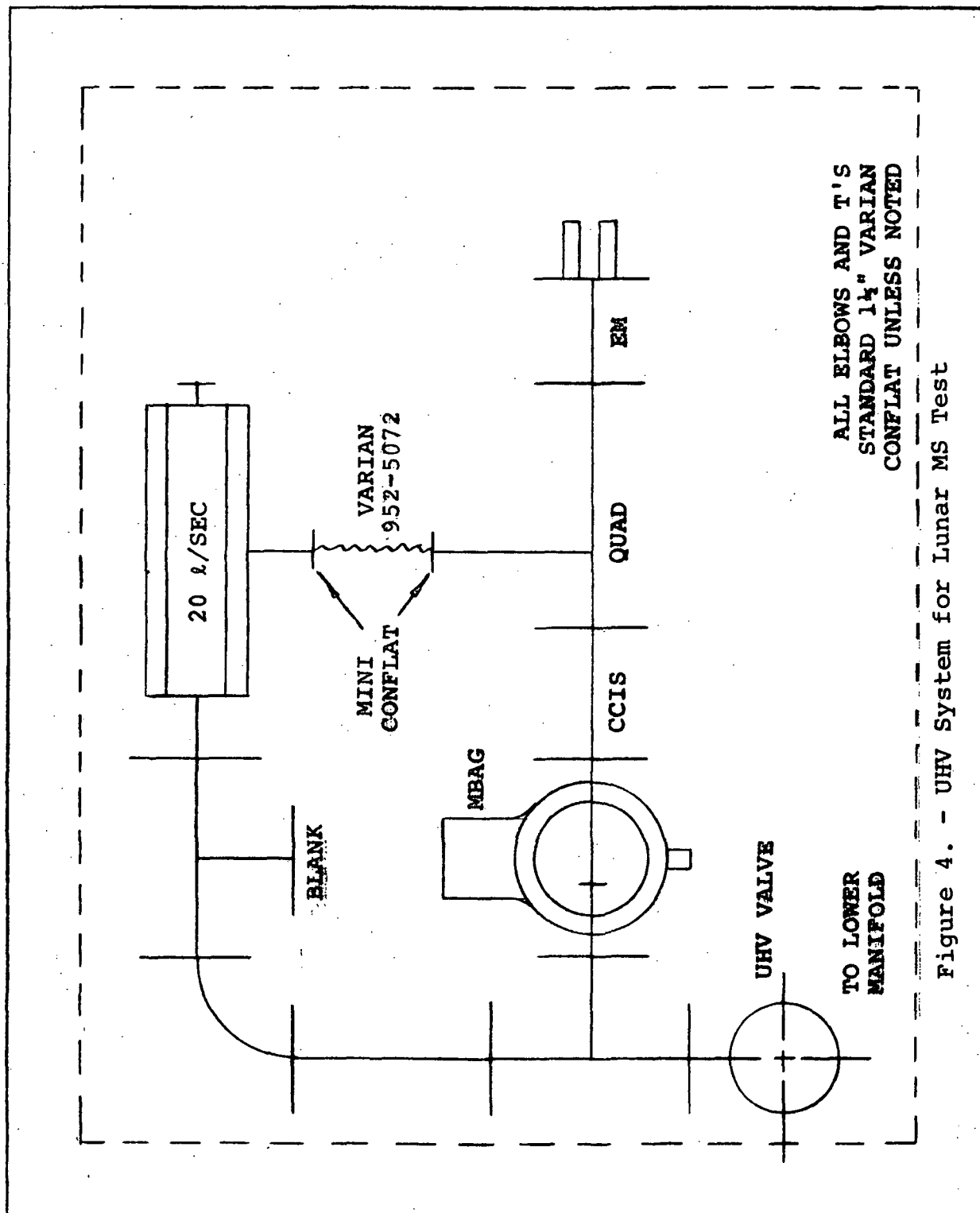
Figure 5.— EXPERIMENTAL TEST VACUUM SYSTEM.

The assembled system (less CCIS/Quad) was baked over-
night at 350°C to reduce the major outgassing sources. The
system was next back filled with dry N_2 gas and the
CCIS/Quad attached. The system was then ready for normal
bake-out and pumping procedures.

This work concluded the modification and preparation of
the CCIS/Quad and test vacuum system. The next section will
describe the in house test procedures and results.

IN HOUSE TEST PROGRAM

Procedures and Results

General Procedures. - Prior to admitting the test gases,
the UHV section of the vacuum system was baked at 350°C
for approximately 24 hours. Immediately following the bake-
out, the modulated Bayard Alpert gauge (MBAG) was outgassed
by electron bombardment at approximately 150 watts for an
hour or so. The UHV valve between the upper (UHV) and lower
manifold was then closed and the system allowed to pump down
into the 10^{-11} Torr range.

Electronic Equipment. - The data to be presented herein
were obtained using both ion pulse counting techniques and
dc ion current measurements. The latter method was used
primarily to extend the dynamic range of measurement beyond
the capabilities of the laboratory digital/analog converter.
This D/A converter will only display a range of approximately
100:1 without manually changing the range. The logarithmic
electrometer can readily display variations in peak height
as large as 10^5:1, without switching.

22

Before obtaining the required test data, certain adjustments were made to the quadrupole drive electronics, the purpose of which was to operate the analyzer in the so called "constant Δm" mode. A detailed description of these adjustments is given in the APPENDIX section of this report. Other discussions will also be given in conjunction with the test results.

In connection with the use of ion counting techniques, two different types of preamplifier-discriminators were employed. The preamplifier used to obtain data in accordance with the contract test procedures is a miniaturized[*] unit whose output pulses are of constant amplitude and peak shape. The input of this preamplifier is sensitive to total charge per input pulse. The internal discriminator may be varied in sensitivity over a range of 3×10^4 to 1×10^6 electrons, according to the manufacturer. A non-linear relationship exists between the input charge sensitivity and an arbitrary test point voltage used to set the discrimination level. A calibration curve of input charge sensitivity vs. test point voltage (discriminator setting) was supplied.

The other type of pulse preamplifier[†] is a linear pulse amplifier with a voltage gain of 100. All pulses are amplified by the fixed voltage gain of 100, provided the resultant output pulse does not exceed 10.00 volts (0.10 volts at the input). The specified sensitivity of this preamplifier is 2.4×10^{-13} coulombs per volt output. Thus, a 50 millivolt

---

[*] Johnston Laboratories, Inc. Model PAD-1, Preamplifier Discriminator.

[†] Hewlett Packard Model 10615A.

output pulse corresponds to an input peak charge of 7.5×10^4 electrons. Therefore, the lower limit of sensitivity for the two amplifiers is approximately the same. The linear preamplifier does not contain a discriminator; instead the scaler used to count the pulses has a built in discriminator which is calibrated directly in volts from 0.050 to 5.00 volts. The linear preamplifier and scaler discriminator were used to obtain all integral pulse height distribution curves, because the discriminator setting is calibrated directly in volts.

The two preamplifiers were compared using the Ar^{40} peak. The results are shown in Fig. 6. These results were carefully repeated to demonstrate that the 25% difference in plateau counting rates was real and not due to variations in the argon partial pressure. The difference in plateau counting rates appears due to the fact that the PAD-1 output pulse width is approximately one-tenth (0.25 µs) the pulse width of the linear preamplifier ($\simeq 2.5$ µs). The PAD-1 preamplifier also appears to be slightly more sensitive, as mentioned above. It is important to note that the resolution loss of the PAD-1 preamplifier becomes noticable at counting rates above 2×10^5 ions/second. For example, it can be shown that a resolution loss (random events) of 5% will occur at the above rate if the resolving time of the preamplifier is 0.25 µ sec as specified. Therefore under the test conditions to be described, a small resolution loss ($\simeq 5\%$) will accompany counting rates of the order of 2×10^5 ions per second.

24
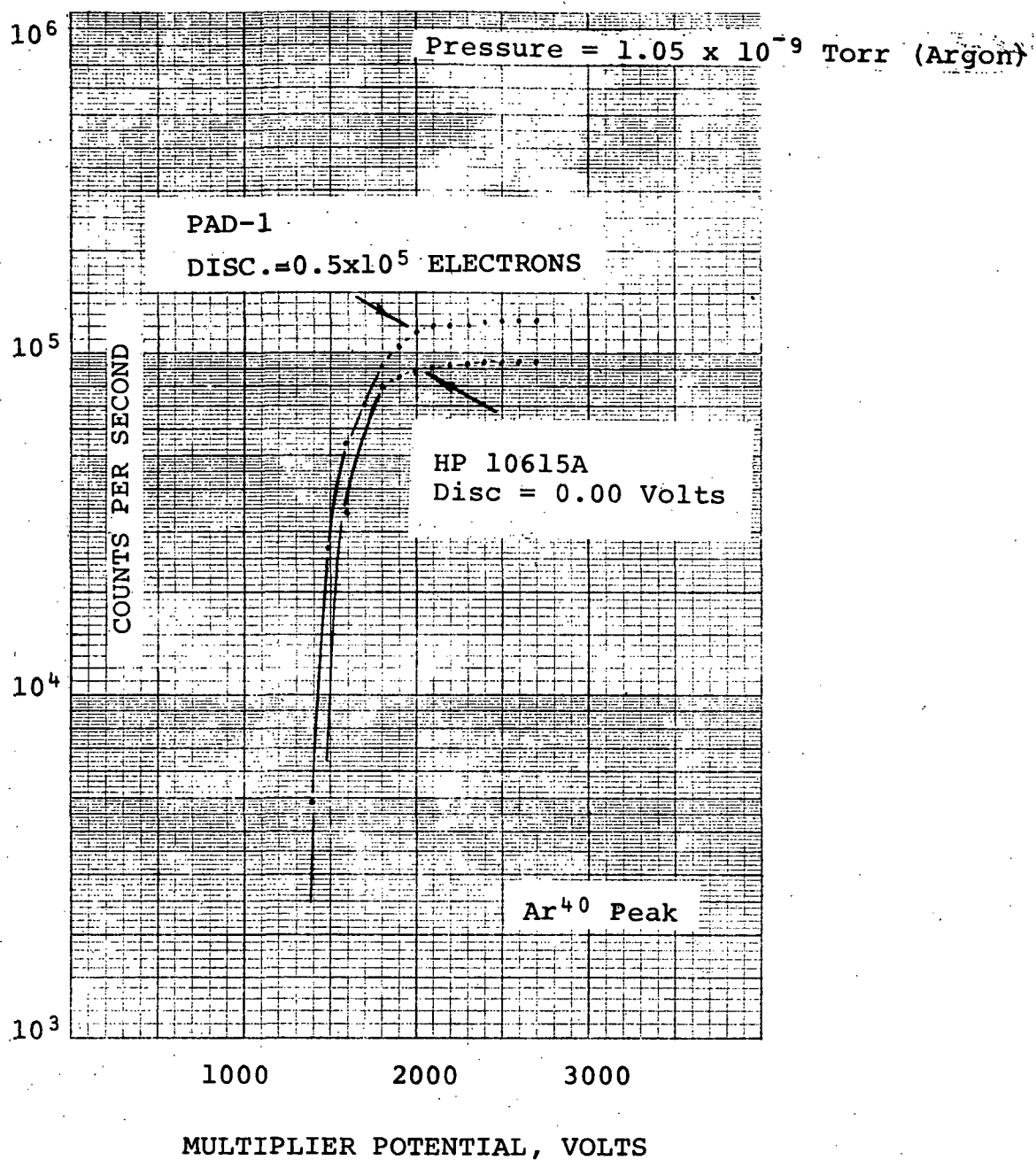
Figure 6. - Counting Rate Comparison of Two Preamplifiers.

Preliminary In House Test Results

Analog and Digital Spectra. - The following comments
and data are presented to verify the CCIS/Quad performance
as set forth in the contract work statement tests objectives
and procedures outlined in pages 5 thru 8.

Figures 7 thru 9 demonstrate the overall instrument
performance with respect to the design goals and test pro-
cedure requirements. Figure 7 shows a digital spectrum
taken on the 1-50 amu range using a mixture of inert gases
and system residuals. The sensitivity of the D/A converter
has not been changed to detect the numerous small peaks
which are not displayed within the limited dynamic range of
the converter. Figure 8 displays the CCIS/Quad's dynamic
range much more effectively. The peak counting rates of
selected mass are also noted on this figure. The multiplier
voltage used for the counting data was set so that all ions
in the mass range were counted, as will be demonstrated
shortly. The multiplier voltage used for the logarithmic dc
current spectrum was purposely set to a lower value to minimize
statistical fluctuations on the smallest peaks. Below
approximately 10^{-12} amperes, the time constant of the logarith-
mic electrometer influences the apparent width of all peaks.

Some caution must be exercised in analyzing this data.
First, the current scale is logarithmic and covers a dynamic
range of 10^5. Secondly, although the inert species, Neon and
Argon are clearly evident, the presence of doubly ionized
species may preclude the accurate determination of isotope
ratios for these gases. Mass 20 undoubtedly includes both

26

Fig. 7 PULSE COUNTING SPECTRA
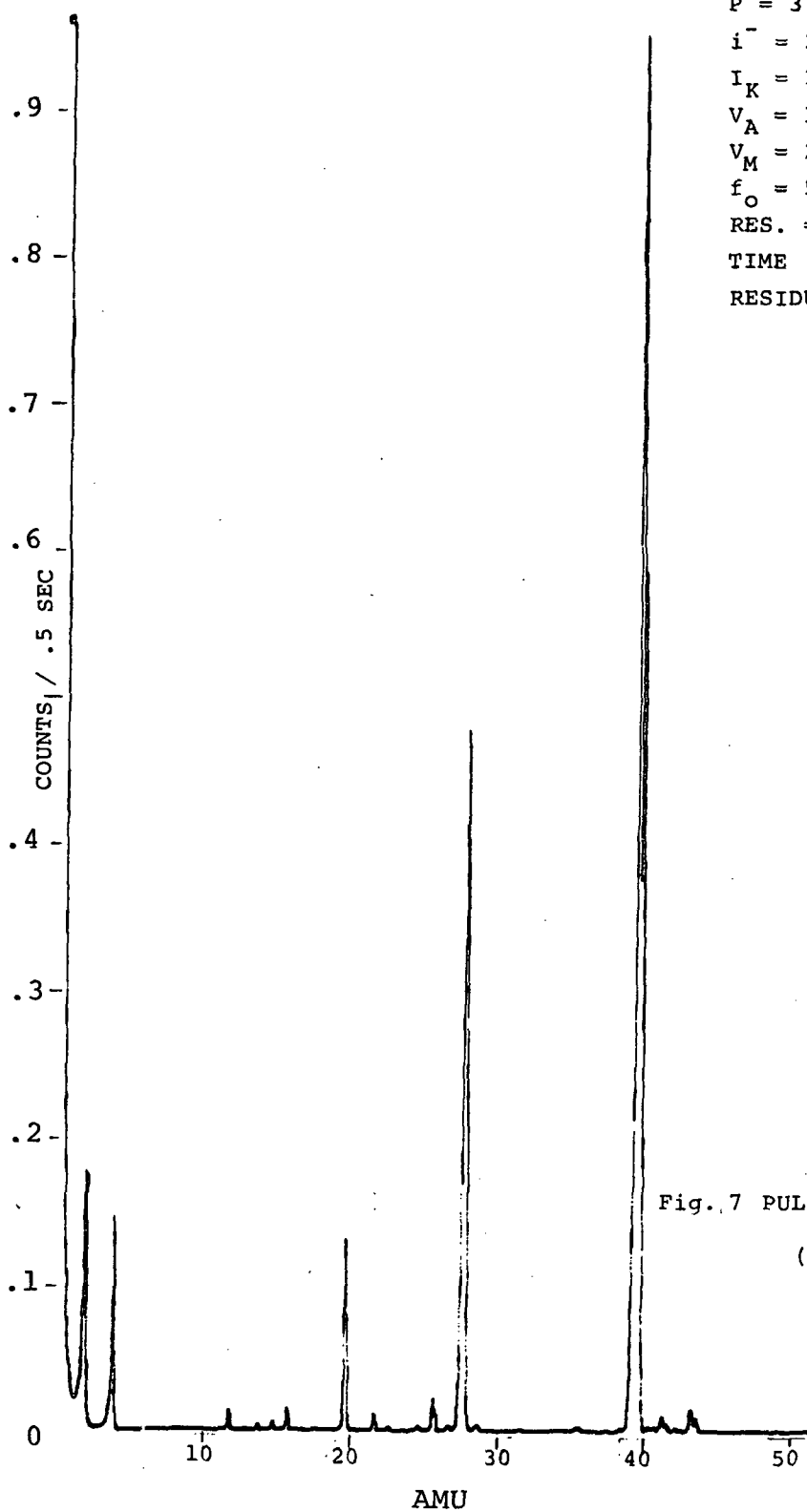
(LOW RANGE)

$P = 3.3 \times 10^{-9}$ TORR

$i^- = 2.35$ ma

$I_K = 3.2 \times 10^{-9}$ AMP

$V_A = 1000$

$V_M = 2300$

$f_o = 5.8$ Mhz

RES. $= 7.64$

TIME 14 min 32 sec.

RESIDUALS + GAS MIXTURE

27

Ne^{20} and doubly ionized Ar^{40}. Similarly, mass 22 is likely to include both Ne^{22} and doubly ionized CO_2. The argon isotopes, Ar^{36} and Ar^{38} appear to be in good agreement[*] with published values on a dc current basis. On a counting basis, the agreement is not as good. Other pulse counting isotopic ratio data to be presented later are in better agreement with published values.

Resolution on Low Mass Range. - Figure 8 also demonstrates that the resolution design goal set for the Ar^{40} peak has been met. The intensity of the Ar^{40} peak is less than 1/300 of the peak value at 39 amu and is < 1/1000 of the peak at 41 amu.

Other important observations can be made from Figs. 7 and 8. It can be seen (especially in Fig. 8) that all mass peaks below approximately mass 30 are generally narrower (at the same percentage of peak height) than those above mass 30. This indicates that the sweep circuit is not operating precisely in the so-called "constant Δm mode". As a result the transmission of the quadrupole may be lower for the lighter masses than for the heavier masses, as is discussed in detail in the APPENDIX.

Resolution on Medium Range. - Turning now to Fig. 9, the performance achieved on the upper mass range will be described. The major Xenon isotopes (129, 130, 131, 132, 134, and 136) are clearly resolved. Another resolution design goal set for the instrument requires the Xe^{131} and Xe^{132} isotopes to be resolved with a valley between of < 50%. This valley

---

[*]Appropriate corrections must be made for the contribution of Ar^{40} peak to the Ar^{38} peak as suggested by the dotted line in Figure 8.

Fig. 8 LOW RANGE LOG SPECTRA

P=1.8 X 10^{-9} TORR
$i^- = 2.35$ ma
$I_K = 2.0$ X10^{-9} AMP
$V_A = 1000$
$V_M = 1600$ LOG SPECTRA
$V_M = 2500$ COUNTING DATA
$f_O = 5.8$ Mhz
RES = 7.64
RESIDUALS + ARGON

FIG. 9 PULSE COUNTING SPECTRA (MED. RANGE)

RESIDUALS + GAS MIXTURES

$P = 2.8 \times 10^{-9}$ TORR

$i^- = -.35$ ma

$I_K = 3.0 \times 10^{-9}$ AMP

$V_A = 1000$

$V_M = 2300$

$f_o = 3.98$ Mhz

RES $= 6.52$

TIME 51 MIN. 32 SEC.

$5 \times 10^3 / .5$ SEC.

COUNTS/.5 SEC.

ATOMIC MASS UNITS

10×10^4

is 35% of the 132 peak and 40% of the 131 peak. This requirement has therefore been met. A third resolution design goal requires less than 1% contribution at mass 135 from the adjacent peaks at 134 and 136 amu. This requirement has not been met. The contribution of each peak to the valley between appears to be approximately 3%. However, it can be seen that major isotopes have been well resolved and that the minor ones (128 and 130) are also evident.

Sweep Time. - Another design goal specified for the instrument requires the total sweep time from mass 1-150 amu to be less than one hour. The sweep time to scan the 0-50 amu range was 14.53 minutes (see Fig. 7). The sweep time to scan 0-150 amu range (Fig. 9) was 51.53 minutes. If the latter scan covers the range from 45-150 amu, the time would be 0.343 x 105 = 36 minutes. The total scan time would therefore be:

0-50 amu	14.53 minutes
45-150 amu	36.00 minutes
Total	50.53 minutes

Obviously, a small additional amount of time would be required for changing mass range and transmitting associated housekeeping data, which would result in an overall sweep time of approximately 51 minutes.

Detection Efficiency vs. Mass. - It was stated previously that tests were conducted to demonstrate that all ions within the mass range 1-150 amu were collected and detected by the multiplier and counting electronics. Figure 10 shows how the counting rate for the inert ions varies as a function of multiplier voltage. It will be seen that for
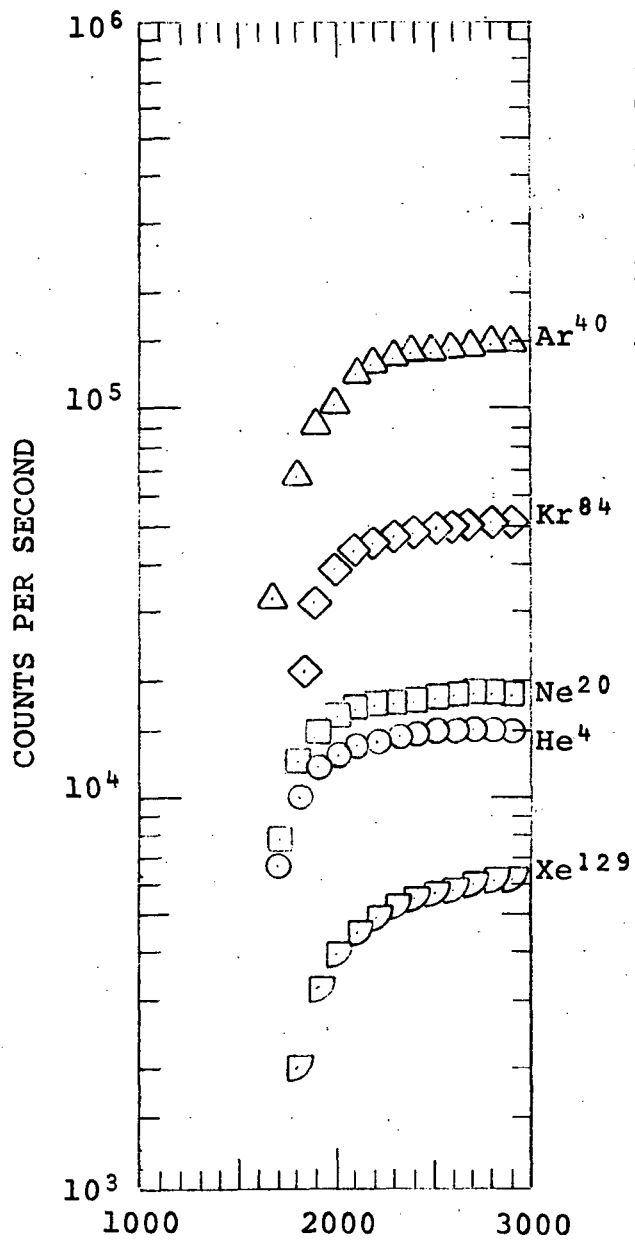
Linde Gas Mixture
TAW #1225
Pressure $\simeq 2.7 \times 10^{-9}$ Torr (Ar)
$I_K = 3 \times 10^{-9}$ Amp
PAD-1 Discriminator 0.5×10^5
                                    Electrons
$V_A = 1000$ Volts

Figure 10. - Counting Rate vs. Multiplier Potential.

He, Ar and Kr, the increase in counting rate for a 600 volt increase in multiplier voltage (2300 to 2900 volts) is 10% or less[*]. For Xe, the increase is about 12%. Thus, the multiplier voltage (and discriminator settings) chosen for Figures 7-9 result in an ion collection and detection efficiency approaching 90%. This number is sufficiently close to 100% (considering experimental errors), that the original pronouncement is essentially correct.

The absolute gain for the inert gases was measured using the dc current and counting rate data as described in ref. 3. The results are listed in Table I below:

TABLE I

Calculated Gains for Selected Masses at 2500 Volts

Mass No. AMU	Gain (Low Range)	Gain (Med. Range)
4	1.25×10^7	---
20	1.01×10^7	9.85×10^6
40	7.55×10^6	7.95×10^6
84		6.25×10^6
129		5.93×10^6

Argon Sensitivity and Linearity. - In concluding the in house test program, it was necessary to establish a

---

[*]The multiplier gain for Argon increases by more than ten-fold over this range of voltage.

sensitivity figure for argon, so that a lower limit of partial
pressure detectability can be estimated. Argon was intro-
duced and the MBAG emission current set to measure "equivalent
Torr argon". Complete spectra where taken from 1-50 amu for
each point shown in Figure 11 to evaluate the effect of other
gases on the argon sensitivity measurement. During the initial
part of the run (lowest pressures), the mass 28 peak (probably
CO^+) was approximately 50% of the argon peak height. As more
argon was introduced, the mass 28 peak continued to increase
but at a slower rate. Presumably, CO was being desorbed as
argon was admitted; the ion pump being a likely source of this
problem. In any event, the resulting argon sensitivty value
is probably slightly low because of the presence of mass 28. The
measured sensitivity for the argon 40 peak obtained from
Figure 11 data is

$$S_{ar} = 2.5 \times 10^{14} \text{ pulses/sec/Torr (Argon)}$$

Sensitivity for Other Gases.- Although the composition
of the inert gas mixture used in Figures 7 and 9 is well known,
it is not possible to use it to obtain accurate sensitivity
figures for the other inert gases, having once determined the
absolute sensitivity for argon. The reason lies in the method
used to introduce the gas into the ultrahigh vacuum section of
the test system. The gas mixture in the lower manifold is
maintained at relatively high pressure (a few Torr). Accordingly,
the mixture enters the UHV section of the system under transition
flow conditions, which may effect the flow rate for individual
species. This problem, combined with the variable pumping

34
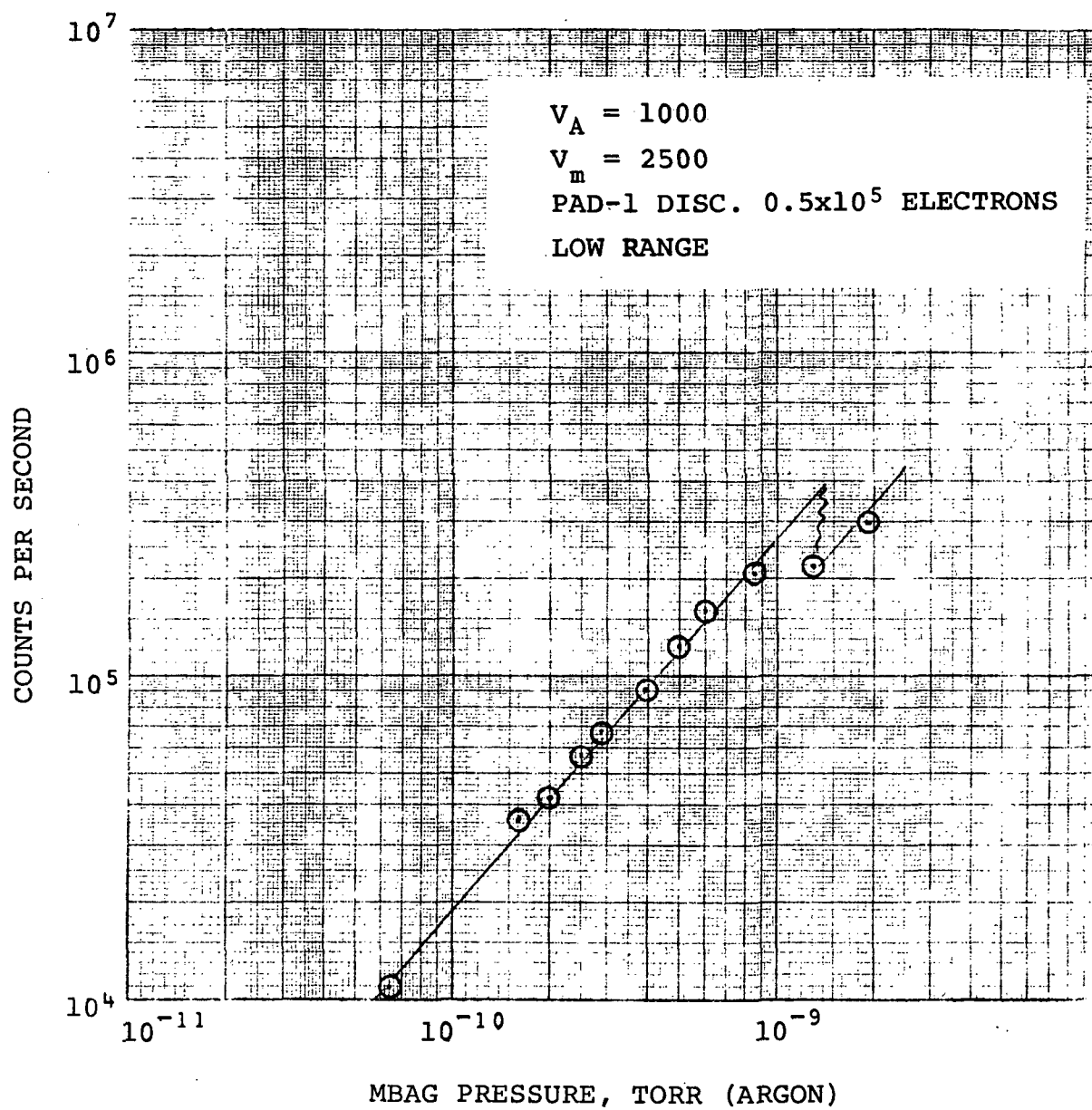
Figure 11. - Argon Counting Rate Sensitivity Calibration

speed of the ion pump for each constituent alters the gas composition within the test system. To improve the sensitivity determinations, each gas was introduced separately and the sensitivity determined individually. This will be discussed in the next section of the report.

Power Estimates. - Based on the measured performance of the CCIS/Quad described in ref. 5, the power requirements for a flight version of the CCIS/Quad Lunar Mass Spectrometer can be estimated with reasonable accuracy and confidence. The necessary calculations and measured operating parameters are described and discussed in the APPENDIX.

The final section of the report will outline certain additional UHV tests conducted by the contractor in lieu of the molecular beam facility tests originally planned but not performed. The major thrust of this work was to establish a minimum detectable partial pressure for selected inert gas species, using the small UHV system described herein. This system, with thorough baking and outgassing is capable of achieving ultimate total pressures in the mid 10^{-12} Torr (nitrogen) range, thus permitting extension of the measurement made during the in house test program to lower pressures.

Extended Ultrahigh Vacuum Tests

General. - In lieu of the molecular beam facility tests originally required by the contract work statement, it was proposed that additional tests be conducted at the contractor's

facility in an effort to obtain further information on the minimum detectable partial pressure performance of the CCIS/ Quad Lunar Mass Spectrometer. It was recognized that these tests could not duplicate certain information which would have been obtained from more extensive tests in a well de- signed molecular beam vacuum facility. For example, the out- gassing effects of the CCIS/Quad cannot be unequivocally isolated from other sources of background gas (ion pump, gauge and associated vacuum hardware). Additionally, the MBAG is limited in its ability to measure total pressure accurately, especially near the gauge's x-ray limit[*]. For sensitivity determinations below the lowest pressure measur- able by the MBAG ($\simeq 5 \times 10^{-12}$ Torr), the use of the known isotopes of selected gases is a convenient method. Pro- vided that other species of the same mass number do not interfere with the isotope ratio, the measurement may be extended to values approaching 1×10^{-14} Torr for certain isotopes. Briefly, this method was used in the extended tests to be reported next.

Tests Methods and Procedures. - The test vacuum system remained unchanged between the in house tests and those to be reported next. The vacuum system was baked at 400°C overnight and the MBAG outgassed at 150 watts (grid dissipa- tion) for 3 or 4 hours to clean up the system initially. The system was then permitted to pump down for 24 to 36 hours. During this period the grid voltage on the MBAG was maintained

---

[*]For a complete discussion refer to ref. 8, pp. 323-327.

at 1000 volts dc[†] and the electron emission current was set at its nominal value of 2.8 milliamperes. This procedure prevents adsorption of gas on the grid which yields erroneous readings below approximately 2×10^{-11} Torr. A digital electrometer was utilized to read the ion currents during modulation of the gauge. The modulated gauge was shrouded to prevent photo emission from the ion collector and a small fan was placed near the glass bulb to reduce outgassing.

To determine true pressure using the MBAG it is first necessary to establish the true x-ray limit of the gauge. Once this value has been determined, the modulation technique may be utilized, (1) to establish that the gauge is clean enough to read system pressure and (2) to measure the unknown pressure. The x-ray limit was measured by plotting ion collector current as a function of grid voltage. To insure that the MBAG grid was not desorbing gas during the measurement, the grid potential was set at 1000 volts (3 ma emission) and left in this condition overnight. The x-ray limit was then determined by reducing the grid voltage (emission constant) from 1000 to 100 volts. The x-ray limit at normal grid voltage and emission current was determined by extrapolation of the x-ray photoelectric response curve. The residual current was also measured by modulating the MBAG and this value checked closely (5%) the value determined by direct measurement. The x-ray limit for this gauge is 1.8×10^{-11} Torr nitrogen equivalent. The system residual pressure, obtained from modulation data, was 9×10^{-12} Torr.

[†]The grid voltage was returned to its normal value of 150 volts above ground to make pressure readings.

Before the introduction of each test gas, the x-ray limit was established by direct measurement and also by modulation. Background spectra (digital) were taken to establish base-line conditions. Figure 12 displays one of these spectra taken at an equivalent "nitrogen pressure" of 9.7×10^{-12} Torr. The hydrogen peak is the most prominent, with mass 28 (CO and N_2), CO_2, Ar and the methane series as minor peaks. It should not be inferred however, that hydrogen has the largest number density of all the gases displayed in this spectra. The sensitivity for this gas (and others such as CO and methane) has not been evaluated. Suffice it to say, that hydrogen is certainly a major constituent and quite possibly has the largest partial pressure. Furthermore, it is also to be expected that the residual hydrogen pressure would be larger than that calculated in the APPENDIX since no hydrogen sources external to the CCIS/Quad were postulated in these calculations.

Argon Results. - Before admitting argon, the system background pressure (argon equivalent)* was 8.2×10^{-12} Torr. The background spectra (shown in Fig. 12) displays a mass 28 peak nearly four times larger than the mass 40 peak. The hydrogen peak is about one-third of the mass 28 peak. After slowly admitting argon, the mass 40 peak increased from 150 cps to 1600 cps or a factor of 10.7. The hydrogen and CO_2 peaks did not change measurably, while the 28 and 16 peaks increased by 30% and 50% respectively.

---

*MBAG argon readings are derived from nitrogen equivalent readings by multiplying by 0.84.

1.0×10^4

.9 —

.8 —

$$P = 8.2 \times 10^{-12} \text{ (ARGON)}$$
$$I_K = 2.65 \times 10^{-12} \text{ AMPS}$$
$$V_A = 1000$$
.7 —
$$V_M = 1800$$
$$RES = 7.64$$

.6

.5

.4

.3

FIG. 12 BACKGROUND SPECTRA

.2

.1

COUNTS/SECOND

10^4 cps FULL SCALE

10^3 cps FULL SCALE

0   10   20   30   40   50

AMU
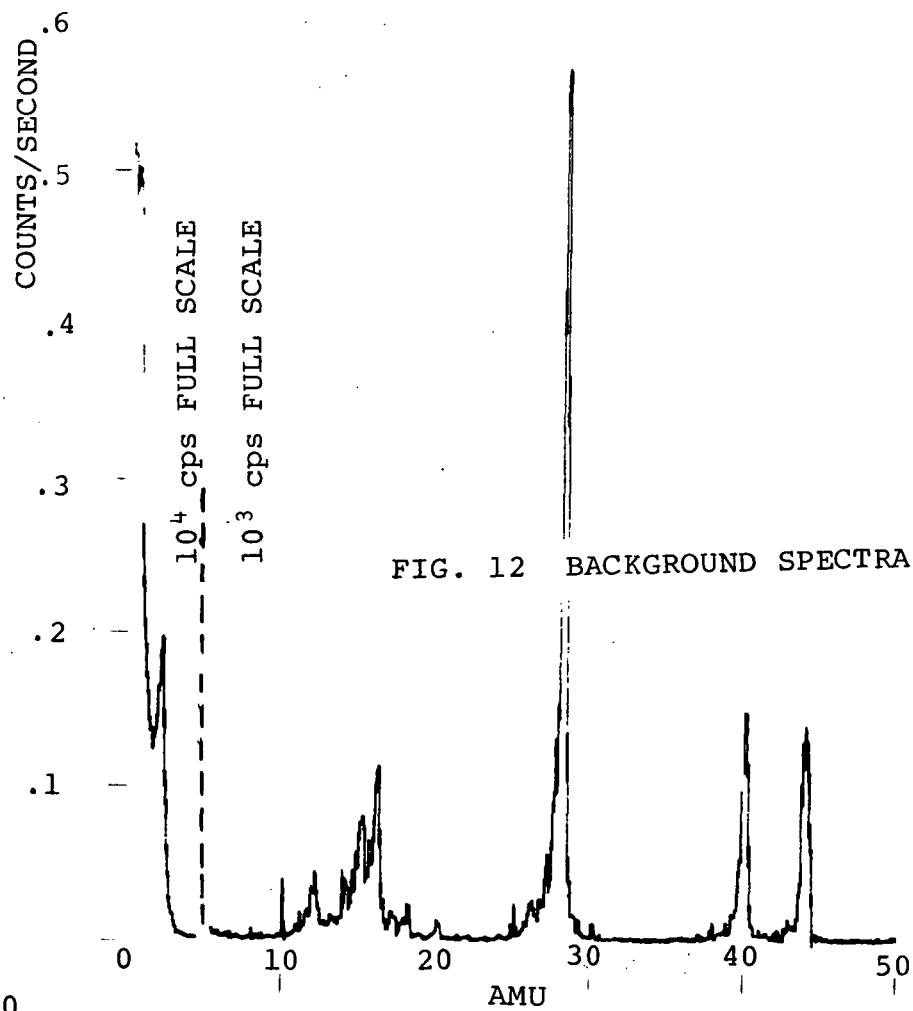
Upon admitting argon, a very small peak was observed
at mass 36 which was about twice as large as the background
noise (8 cps vs. 4 cps). The equivalent argon pressure as
recorded by the MBAG was 9.25×10^{-12} Torr. Neglecting the
hydrogen peak momentarily, and totalizing all Ar^{40} ions
(singly and doubly ionized) the net change in these peaks
totalled 1535 cps. The hydrogen peak was 1960 cps and the
mass 28 peak was 740 cps (about 50% of Ar). Again neglecting
hydrogen and the minor peaks, we approximate the true argon
partial pressure by assuming that the nitrogen and argon
sensitivities (cps/Torr) are approximately equal. It then
follows that

$$P_{total} = P_{Ar} + P_{N_2} \quad \text{where} \quad P_{N_2} \simeq \tfrac{1}{2} P_{Ar}$$

Therefore,

$$9.25 \times 10^{-12} \text{ Torr (Ar)} = P_{Ar} \ (1 + 0.5)$$

$$P_{Ar} = 6.2 \times 10^{-12} \text{ Torr}$$

The sensitivity for Ar then becomes

$$S_{Ar} = \frac{1535}{6.2 \times 10^{-12}} = 2.48 \times 10^{14} \text{ cps/Torr Ar.}$$

This value compared favorably with a figure of
2.5×10^{14} cps/Torr previously determined from the data of
Fig. 11.

Returning now to the question of hydrogen and its effect on the MBAG total pressure reading, the digital spectrum shows that the hydrogen peak was small (30%) in comparison with the total number of unresolved ions at mass "zero". Since the quadrupole transmission for hydrogen is large (compared to the heavier masses) and since the ionization efficiency of the CCIS and MBAG for hydrogen is approximately 50% of that for the heavier mass, it follows that the number density of hydrogen may be as large as 50-60% of the total for all other gases. Thus, the sensitivity number quoted above is probably low since the total pressure observed by the MBAG neglects a partial pressure of hydrogen which may be 50% or more of the total pressure.

Without continuing to speculate further, we estimate that the very small argon peak observed appears to correspond to an Ar^{36} partial pressure of

$$P_{Ar^{36}} = 6.2 \times 10^{-12} \times 0.337 \times 10^{-2}$$

$$= 2.1 \times 10^{-14} \text{ Torr } (Ar^{36}), \text{ S/N} \simeq 2:1$$

The observed isotope ratio can be calculated from the data, although the accuracy is admittedly poor because of the low S/N ratio and statistical accuracy. This ratio is $\frac{4}{1535} = 0.0026$.

Thus, it appears that a rough estimate[*] for the minimum detectable partial pressure for Ar^{36} is 2.0×10^{-14} Torr

---

[*]As will be discussed shortly, a more conservative estimate for the minimum detectable partial pressure of argon yields a value of 4×10^{-14} Torr (argon).

as determined by the actual argon pressure measurement near 6×10^{-12} Torr. This estimate neglects a noticable hydrogen background, as well as contributions from the minor constituents.

In a series of three additional experiments the argon partial pressure was slowly increased to improve the S/N ratio. Table II summarizes the counting rate data for the major and minor peaks and also the "zero mass" rates for all argon runs. No corrections have been made for background noise or for the effect of gas composition on MBAG readings.

TABLE II

SUMMARY OF SPECTRAL DATA FOR ARGON
(Thousands of counts/sec)

Run No.	Zero Mass	2	16	20	28	36	40	44	Pressure Torr Ar
1	5.2	2	.114	.015	.57	.004	.15	.14	8.2×10^{-12}
2	6.5	1.96	.170	.100	.74	.008	1.6	.15	9.25×10^{-12}
3	8.5	2.3	.143	.155	.88	.150	2.9	.16	2.34×10^{-11}
4	>10	4.5	.250	.150	8.25	.018	4.6	.25	6.55×10^{-11}
5	>25	4.33	.265	.740	3.0	.073	19.8	.27	1.10×10^{-10}
ΔR		2.16	2.32	50.0	5.27	18.0	132	1.93	13.4

(Not corrected for background noise or variations in gas composition in the MBAG)

$$\Delta R = \frac{\text{Run } 5}{\text{Run } 1}$$

The "ΔR" ratio denotes the factor by which each mass increased as the argon pressure increased. It will be observed that the Ar^{40} peak increased by a factor of 132 times. Mass 28 increased by a factor of five and mass 44 by less than a factor of two. Ar^{++} (Mass 20) and Ar^{36} both increased substantially as would be anticipated. The first two runs have been discussed above: Run 1 represents Figure 12 data, while Run 2 data was used to determine the minimum detectable partial pressure of Ar^{36} discussed previously.

Run 4 was performed before the other runs. During this experiment, an excessive amount of argon was accidentally admitted, together with some CO or nitrogen, causing the mass 28 peak to be larger than the mass 40 peak. The other runs were made in sequence. It will be noted that Run #5 has the largest ratio of the Ar peak to the mass 2 and mass 28 peaks and therefore should be the most reliable in terms of an accurate determination of the true argon sensitivity. Figure 13 displays the digital spectrum obtained for this argon run. The spectrum is shown for two sensitivities of the D/A converter which are a factor of ten apart. The argon total pressure measured by the MBAG was 1.11×10^{-10} Torr. The Ar^{36} peak is clearly discernable. The data shows that the Ar^{36} peak (including noise and the Ar^{40} contribution) was 75 counts/sec. The main argon peak was 1.980×10^3 cps. The isotopic abundance of Ar^{36} is 0.00337. From this, we may calculate the partial pressure of Ar^{36}, assuming that the MBAG reading represents the true total pressure of argon. The Ar^{36} peak then represents a partial pressure of

44
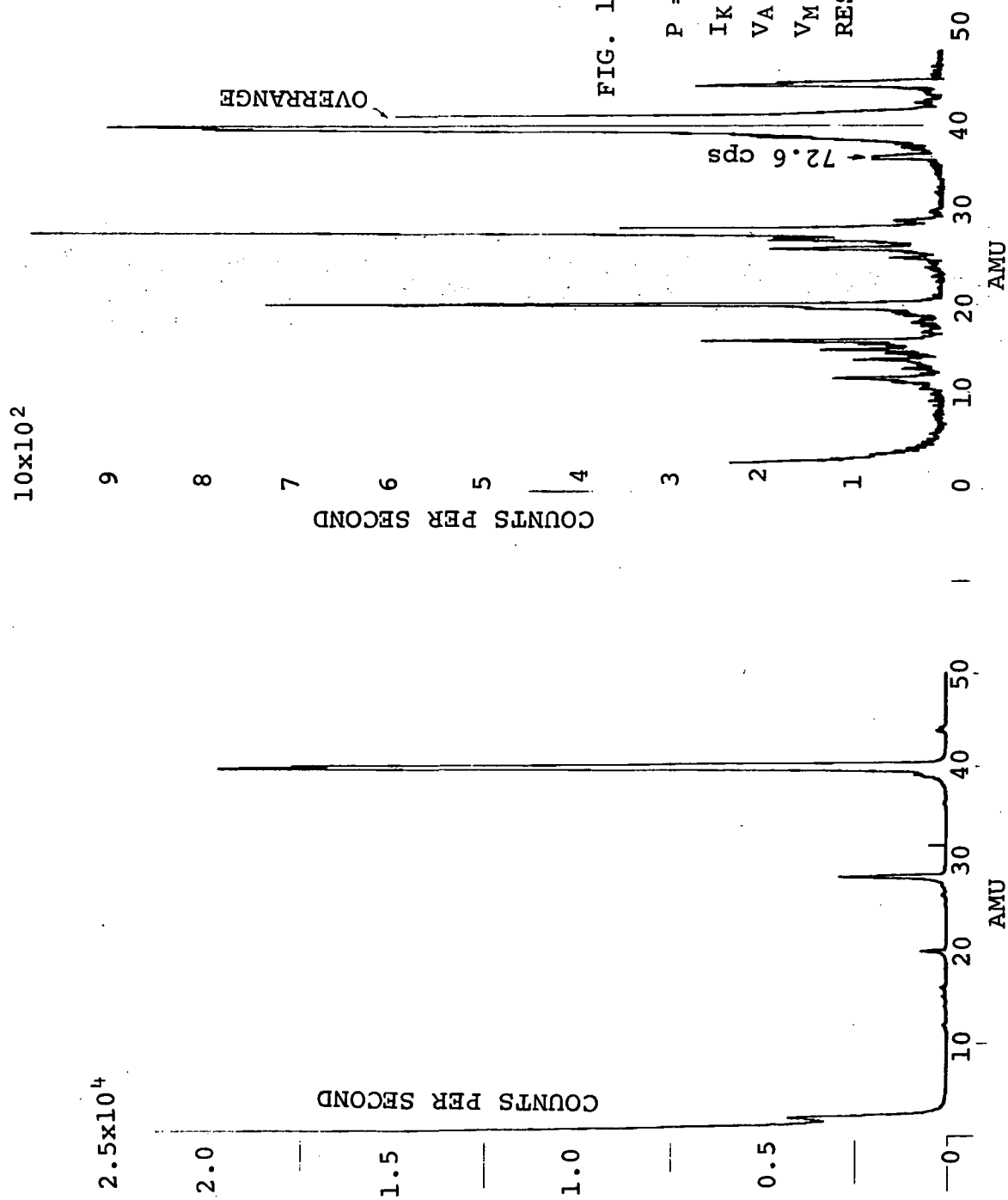
FIG. 13 ARGON AND RESIDUALS

$P = 1.11 \times 10^{-10}$ TORR ARGON

$I_K = 5.0 \times 10^{-11}$

$V_A = 1000$

$V_M = 1800$

RES $= 7.64$

OVERRANGE

~72.6 cps

10×10^2

COUNTS PER SECOND

9 8 7 6 5 4 3 2 1 0

AMU

0 10 20 30 40 50

2.5×10^4

COUNTS PER SECOND

2.0 1.5 1.0 0.5 0

AMU

10 20 30 40 50
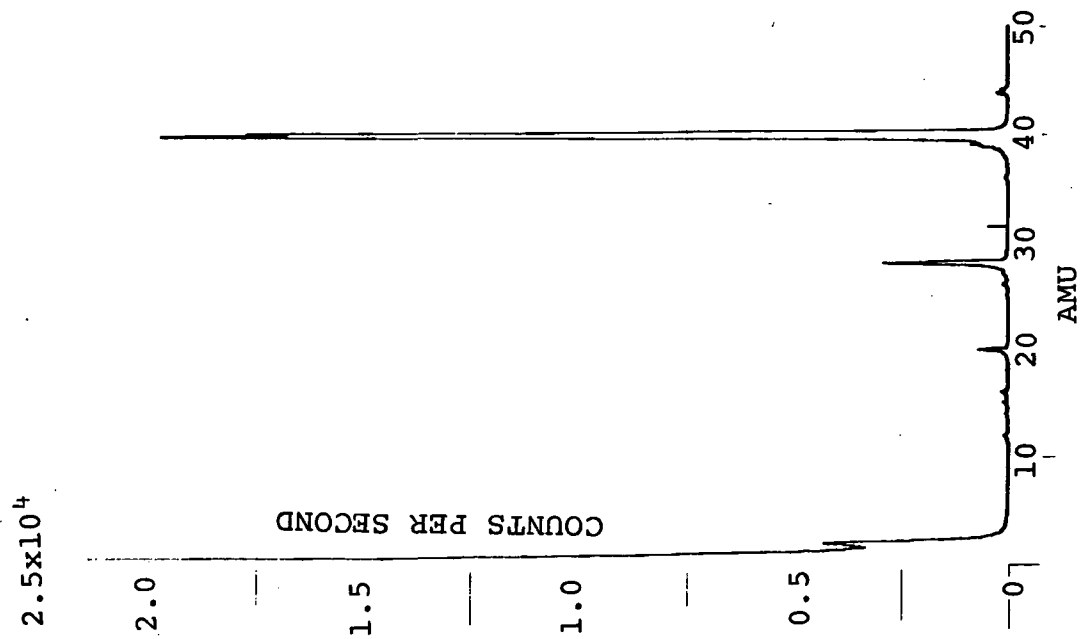
$$Ar^{36} = 1.11 \times 10^{-10} \times 0.00337 \text{ Torr}$$

$$= 3.74 \times 10^{-13} \text{ Torr} \quad S/N \simeq 16:1$$

The sensitivity for Ar^{40} is derived, in the manner described previously, by neglecting the partial pressure of hydrogen, which is small here, and correcting for the mass 28 partial pressure by assuming that the sensitivity of the CCIS/Quad for nitrogen and argon are approximately the same. If this is done, the MBAG reading becomes $1.11 \times 10^{-10}/$ $1.15 = 0.96 \times 10^{-10}$ Torr. The total Ar^{40} counting rate is 2.05×10^4 cps (singly and doubly ionized). The sensitivity for Ar^{40} is therefore

$$S_{Ar} = \frac{2.05 \times 10^4}{0.96 \times 10^{-10}} = 2.14 \times 10^{14} \text{ cps/Torr}$$

Thus, the sensitivity figures derived from data taken over a wide range of argon pressures agree reasonably well, as is recapitulated below:

$$6.2 \times 10^{-12} \text{ Torr} = 2.48 \times 10^{14} \text{ cps/Torr}$$
$$9.6 \times 10^{-12} \text{ Torr} = 2.14 \times 10^{14} \text{ cps/Torr}$$
$$8.7 \times 10^{-10} \text{ Torr} = 2.38 \times 10^{14} \text{ cps/Torr} \quad (\text{Fig. 11 data})$$

The data of Fig. 13 may also be used to calculate the Ar^{36}/Ar^{40} isotope ratio. To make this computation, the singly

46

and doubly ionized Ar^{40} components are again added. The small contribution of the mass 40 peak to the mass 36 peak is subtracted (including photon noise). The isotope ratio is then

$$Ar^{36}/Ar^{40} = \frac{73 - 10^*}{(1.975 + .075) \times 10^4}$$

$$= \frac{63}{2.05 \times 10^4} = 0.00308$$

This value is within 10% of the published figure of .00337 for the ratio.

The S/N ratio for the Ar^{36} data of Fig. 13 is defined as the net Ar^{36} ions divided by the true noise level. This noise is about 4 cps (photons). The net Ar^{36} signal is 63 cps. The S/N ratio is therefore approximately 16:1. In the absence of the main Ar^{40} peak, a small peak similar to that seen at mass 30 (Figure 13) could be detected. Therefore, the minimum detectable partial pressure for argon at 2:1 S/N is approximately $1/8 \times 3.74 \times 10^{-13}$ Torr or about $4.7 \times 10^{-14*}$ Torr.

Summarizing the complete argon information, we note the following:

1. A conservative estimate for the minimum detectable partial pressure, assuming a 2:1 S/N ratio and a noise count of 4 cps is 4×10^{-14} Torr.

---

*The partial pressure of Ar^{36} is derived from an MBAG measurement which includes a minor contribution (15%) from CO and nitrogen. Therefore, the value is about 15% high.

2. The sensitivity for argon is between 2.0
    and 2.4 x 10^{14} cps/Torr as determined over a
    total pressure range of 6 x 10^{-12} Torr to
    9 x 10^{-10} Torr.

3. The evaluation of the instrument's linearity
    using the MBAG is difficult below 1 x 10^{-11}
    Torr because of gas composition variations
    and errors associated with MBAG measurements.

Neon Results. - The next gas to be studied was neon. Neon
has three isotopes which are useful in evaluating spectrometer
performance. These isotopes and their abundances are listed
below:

Ne^{20}	0.9092
Ne^{21}	0.00257
Ne^{22}	0.0882

Because of the relatively low abundance of Ne^{21}, it was
originally planned to utilize this isotope as a means of
determining and demonstrating the lower limit of detectability
for neon. As will be discussed shortly, the experimental re-
sults show that to resolve Ne^{21} properly, an unsatisfactory
trade-off would have to be made between sensitivity and resolu-
tion. As will be discussed, this compromise should stress sen-
sitivity rather than resolution.

Figure 14 displays a digital spectrum of neon and
residual gases taken at a pressure of 9 x 10^{-11} Torr, neon
equivalent. The Ne^{21} peak is not discernable in the valley

48

FIG. 14   NEON AND RESIDUALS

$P = 1.64 \times 10^{-10}$ TORR NEON

$I_K = 5.1 \times 10^{-12}$

$V_A = 1000$

$V_M = 1900$

RES = 7.64

49
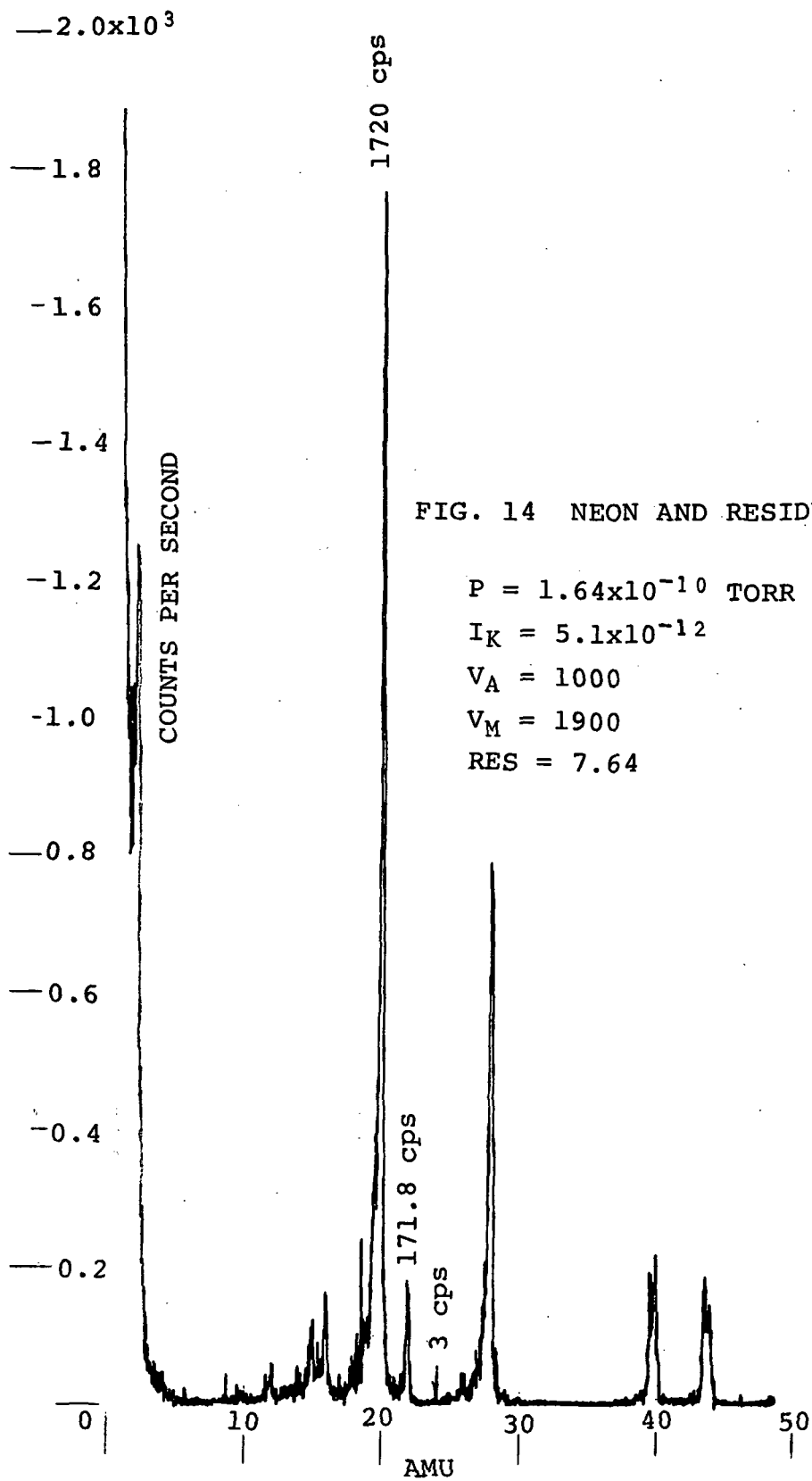
between masses 20 and 21. It can be seen that the ratio
of Ne^{20} to Ne^{22} is in good agreement with the abundance
ratios given above. From this data, the Ne^{20} sensitivity
is computed to be

$$S_{Ne^{20}} = \frac{17.20 \times 10^2}{.909 \times 9 \times 10^{-11}} = 2.1 \times 10^{13} \text{ cps/Torr}$$

Since the Ne^{22} isotope peak is exactly one-tenth of
the Ne^{20} peak, the mass 22 peak represents a pressure of
9×10^{-12} Torr (neon). The S/N ratio for this peak is $\frac{172}{3} =$
57.5. Assuming that a S/N ratio of 2:1 represents a realistic
minimum, then the minimum detectable partial pressure of the
neon isotopes would be $2/57.5 \times 9 \times 10^{-12} = 3.5 \times 10^{-13}$ Torr.

The neon sensitivity is approximately one-tenth the
argon value. Two factors contribute to this result. First,
the total ionization cross-section for neon is appreciably
lower (factor of 4.3) than that for argon. In fact, the cross
section for neon is lower than that for all gases except helium.
The second factor involves the quadrupole sweep circuit char-
acteristics. As shown previously in Figure 8 (and discussed
in the APPENDIX), the mass peaks in the 10-30 amu range are
narrower than those in the vicinity of argon. This signifies
that the quadrupole transmission (sensitivity) for neon ions
is lower than for argon. This factor can be eliminated by
operating the sweep in the "constant Δm" mode which minimizes
transmission variations with mass. The reduced cross section
for neon cannot be corrected. Therefore the neon sensitivity
will always be a factor of four lower than for argon.

Returning to the resolution of Ne^{21}, we also note from the Fig. 8 data that the mass 20 peak[*] begins to interfere with the mass 21 peak at a current of 7.5×10^{-13} amperes. This corresponds to

$$\frac{7.5 \times 10^{-13} \times 100}{1.45 \times 10^{-10}} = 0.52\%$$

of the full peak height at mass 20. Ne^{21} has a percentage abundance of

$$\frac{2.57 \times 10^{-3} \times 100}{.9092} = 0.283\%$$

relative to Ne^{20}. Thus, Ne^{21} could not be observed, because the valley between masses 20 and 21 is nearly twice as large as the full Ne^{21} peak height.

Summarizing this situation it can be seen that a trade-off exists for Ne^{21} which involves increasing the resolving power at the expense of sensitivity (lowered transmission). Since the sensitivity of neon is inherently lower

---

[*]The peaks observed at masses 20 and 22 in Fig. 8 are not neon peaks. They are undoubtedly doubly ionized argon and CO_2, as evidenced by the large ratio of 20/22 peak heights.

than that for all other gases except helium, the practical solution must emphasize sensitivity rather than resolution.

In concluding the discussion regarding neon, Figure 14 shows measurable peaks of hydrogen, CO, Ar and CO_2 which could influence the MBAG total pressure reading used to derive the neon sensitivity. As noted above, the sensitivity for neon is only one-tenth of argon, or stated conversely, a neon partial pressure ten times that of argon, is required to produce equal peak heights of the two gases. Thus the argon contribution, as well as that of CO_2, to the MBAG total pressure readings are negligible. Similarly, it can be deduced that nitrogen is a minor constituent since its cross section is 3.8 times larger than neon and the transmission of nitrogen is between that of neon and argon. Thus hydrogen appears to be the only constituent which could influence the MBAG total pressure readings. Its effect will be to increase the MBAG reading of total pressure from which the neon sensitivity figure is derived. Thus, the neon sensitivity figure of 2.1×10^{13} cps/Torr is a conservative number and the minimum detectable partial pressure derived therefrom is likewise conservative.

52

Krypton Results. - The third gas to be investigated was krypton. Krypton has six stable isotopes with the following abundances:

Kr^{78}	0.00354
Kr^{80}	0.0227
Kr^{82}	0.1156
Kr^{83}	0.1155
Kr^{84}	0.5690
Kr^{86}	0.1737

The relatively low abundance of Kr^{78} and Kr^{80} permits the use of these isotopes in defining a lower limit of partial pressure detectability. After a thorough system bakeout and MBAG outgassing, krypton was admitted to the system. The total pressure measured by the MBAG was 5.5 x 10^{-11} Torr (krypton equivalent). The digital spectrum shown in Figure 15 was obtained. A substantial CO or N_2 peak is evident at mass 28. Neglecting momentarily the mass 28 peak and its

$P = 5.55 \times 10^{-11}$ TORR KRYPTON

$I_K = 4.1 \times 10^{-11}$ AMPERES

$V_A = 1000$

$V_M = 1800$

RES = 6.55

FIG. 15   KRYPTON AND RESIDUALS

54
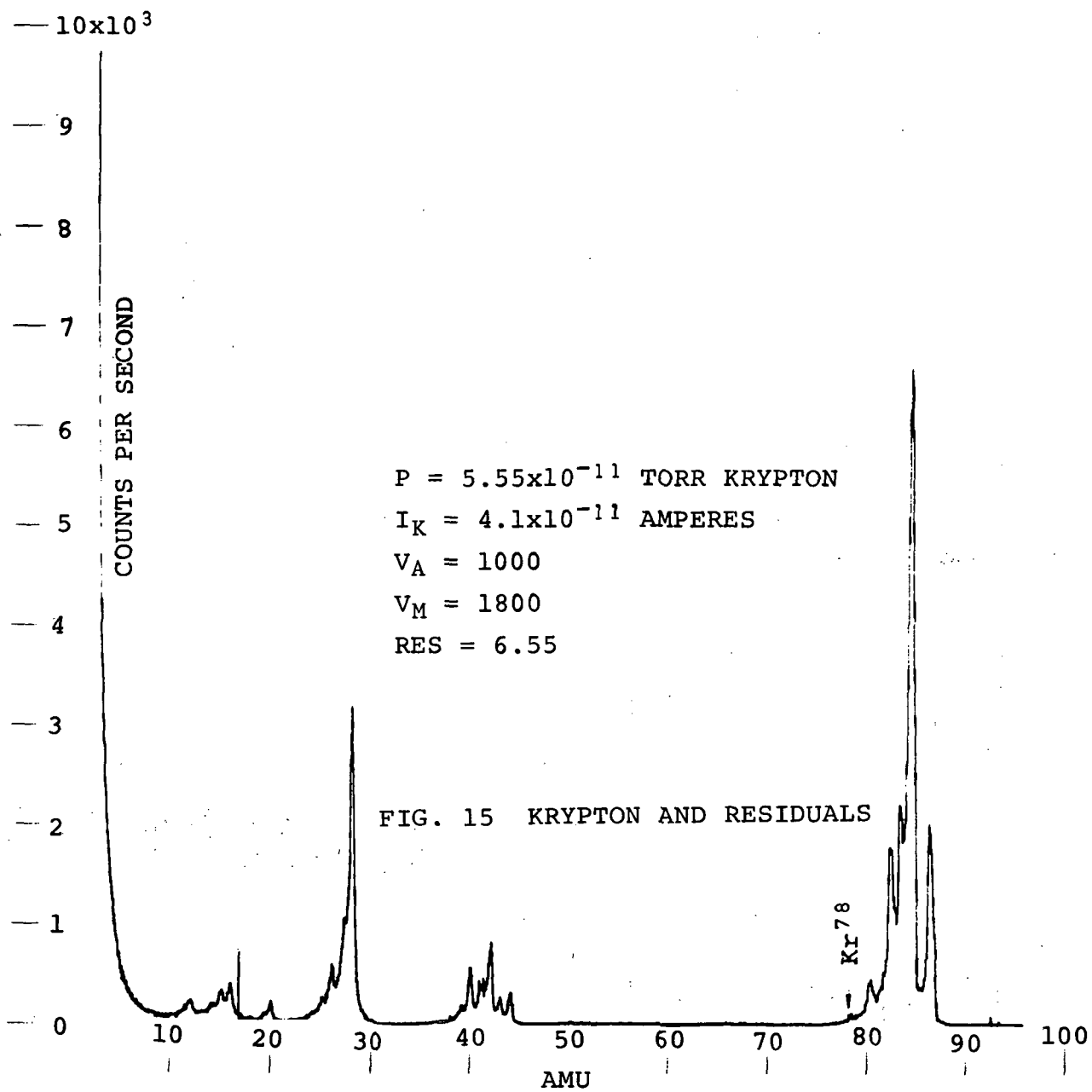
influence on the total system pressure, we calculate the krypton sensitivity as follows:

$$S_{Kr} = \frac{6.6 \times 10^3}{.5690 \times 5.5 \times 10^{-11}} = 2.11 \times 10^{14} \text{ cps/Torr}$$

The Kr^{84} peak represents a partial pressure of $5.5 \times 10^{-11} \times 0.569$ or 3.13×10^{-11} Torr. Similarly, the very small Kr^{78} peak represents a partial pressure of $5.5 \times 10^{-11} \times 3.5 \times 10^{-3}$ or 1.93×10^{-13} Torr. This estimate is conservative in that the influence of the mass 28 peak on the MBAG reading has been neglected. In the previous work (ref. 1), the nitrogen sensitivity of the CCIS/Quad spectrometer was determined to be 1.36×10^{14} cps/Torr. This sensitivity yields a partial pressure of $\frac{3.2 \times 10^3}{1.36 \times 10^{14}} = 2.36 \times 10^{-11}$ Torr for the mass 28 peak of Figure 15. Assuming that the relative partial pressures of krypton and mass 28 are the same in the MBAG and the CCIS and that the ratio of sensitivities of the CCIS and MBAG to the two species are the same, we can estimate the true pressure of krypton in the MBAG. The total ion current (I_T) measured by the MBAG is the sum of two currents, one resulting from krypton and the other from mass 28. The emission current of the MBAG is set to a value which yields a sensitivity of 0.1 Amps/Torr for nitrogen (k_N). The sensitivity of the MBAG for krypton will be 1.66 times* larger than the nitrogen sensitivity. The krypton

---

*Based on the ratio of total ionization cross-sections given in Table 7.2 of ref. 8.

sensitivity will therefore be 0.166 Amps/Torr. With this information the total ion current in the MBAG may be expressed

$$I_T = k_n P_N + k_{Kr} P_{Kr}$$

where P_N and P_{Kr} are the partial pressures of nitrogen and krypton in the MBAG. Substituting the values for P_N and for the sensitivity factors we have

$$I_T = 0.1 \times 2.36 \times 10^{-11} + 0.166\ P_{Kr}$$

The value of I_T actually measured in the Fig. 15 data was 1.03×10^{-11} amperes. Therefore, the krypton partial pressure is

$$P_{Kr} = \frac{1.03 \times 10^{-11} - 0.236 \times 10^{-11}}{0.166}$$

$$= \frac{0.79 \times 10^{-11}}{0.166} = 4.76 \times 10^{-11} \text{ Torr (krypton)}$$

We may now recalculate the true krypton sensitivity of the instrument (accounting for the mass 28 influence) as follows:
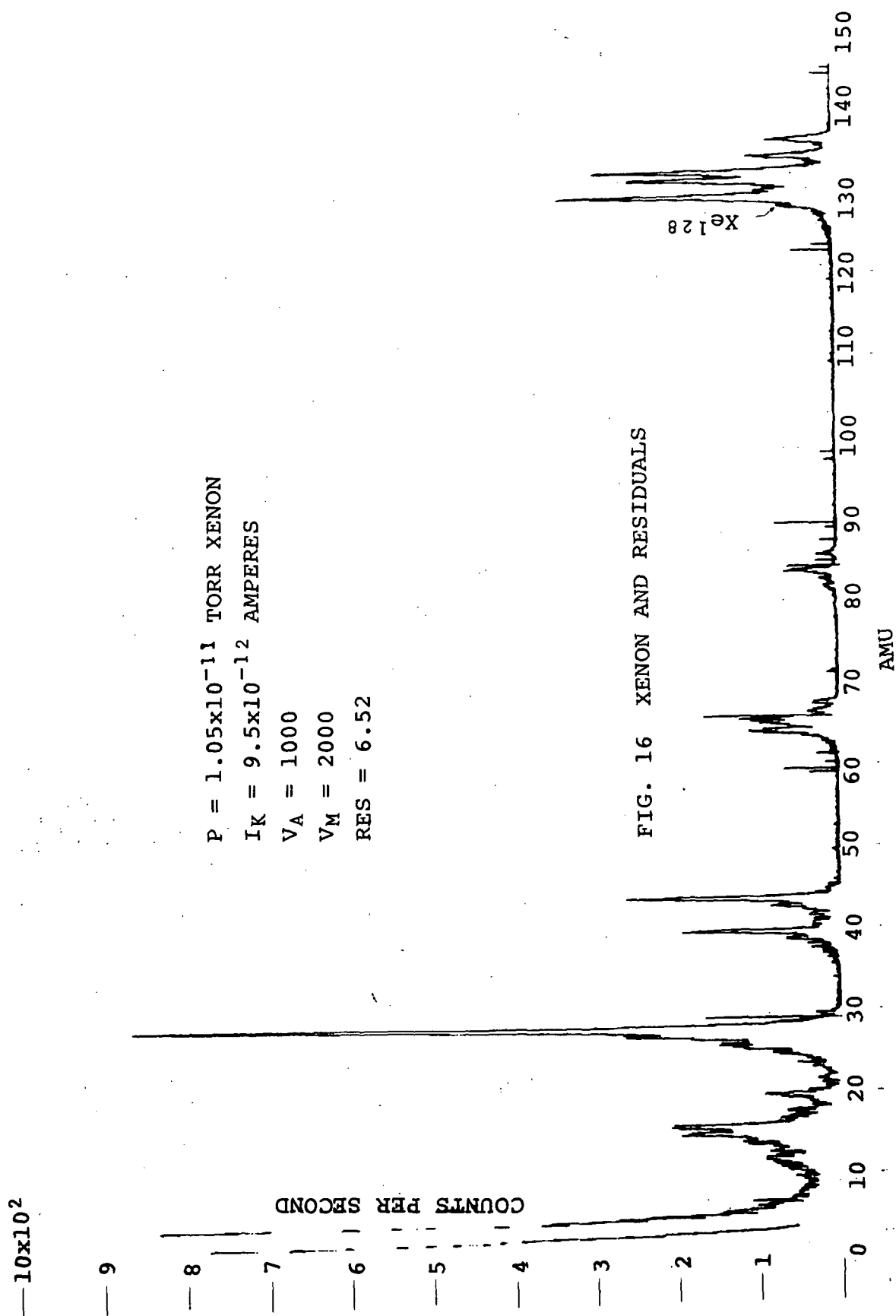
$$S_{Kr}\text{(true)} = \frac{6.6 \times 10^3}{.5690 \times 4.76 \times 10^{-11}} = 2.44 \times 10^{14} \text{ cps/Torr}$$

56

Using this sensitivity, we estimate the Kr^{78} peak to be equal to $3.54 \times 10^{-3} \times 4.76 \times 10^{-11}$ Torr or 1.68×10^{-13} Torr. The background noise level in the vicinity of the Kr^{78} peak is about 9 cps. The S/N ratio at this peak is therefore about 11:1. At a S/N of 2:1, the minimum detectable partial pressure of Kr^{78} would be approximately 3.1×10^{-14} Torr. Thus, the lower limit of detectability at the 2:1 S/N is slightly lower than the value for argon (4.7×10^{-14} Torr).

Xenon Results. - The final gas to be studied was xenon. The spectrometer and vacuum system were baked as before and the MBAG thoroughly outgassed. The xenon isotopes of interest in this experiment are listed below together with their abundances.

Xe^{128}	.01919
Xe^{129}	.2644
Xe^{130}	.0408
Xe^{131}	.2118
Xe^{132}	.2689
Xe^{134}	.1044
Xe^{136}	.0887

A small amount of xenon was admitted to the system and the spectrum shown in Fig. 16 was obtained. Again a prominent mass 28 peak was observed. Correcting for the influence

57

P = 1.05x10^{-11} TORR XENON

I_K = 9.5x10^{-12} AMPERES

V_A = 1000

V_M = 2000

RES = 6.52

FIG. 16   XENON AND RESIDUALS

AMU

COUNTS PER SECOND

10x10^2

Xe128

of this peak on the MBAG pressure reading (as described above for krypton) the true pressure of xenon is calculated to be 1.03×10^{-11} Torr. Thus, the Xe^{128} peak represents a partial pressure of $1.919 \times 10^{-2} \times 1.03 \times 10^{-11}$ or 1.98×10^{-13} Torr. The sensitivity for the xenon isotopes may be calculated (as shown previously)

$$S_{Xe} = \frac{3.4 \times 10^2}{1.03 \times 10^{-11} \times 0.2644} = 1.25 \times 10^{14} \text{ cps/Torr}$$

Finally, in computing the xenon sensitivity and hence the minimum detectable partial pressure of Xe^{128}, the doubly ionized species were omitted, together with minor peaks such as the methane series, Ar and CO_2. Thus the minimum detectable partial pressure estimate for Xe^{128} of 1.98×10^{-13} Torr is conservative. The S/N for this data is certainly > 10:1, which implies a minimum detectable partial pressure at a 2:1 S/N of < 4×10^{-14} Torr for xenon.

In summary, the minimum detectable partial pressure for argon, krypton and xenon are in the realm of 4×10^{-14} Torr for a 2:1 S/N ratio. The minimum detectable pressure of neon is approximately a factor of ten higher, due largely to the very low ionization cross-section of neon.

CONCLUSIONS

The general performance of the CCIS/Quad mass spectrometer has met or exceeded the program design goal specifications established for a candidate lunar atmosphere mass spectrometer. With an average power of less than 8 watts, the

spectrometer resolution and sensitivity are adequate for
analyzing and measuring gaseous species from 0-150 amu
and for partial pressures of the order of 4×10^{-14} Torr.

REFERENCES

1. Torney, F. L., Jr.: Development of a Lunar Mass
    Spectrometer. Final Report for Contract No. NASw-1946,
    NASA, Headquarters.

2. Torney, F. L., Jr., Blum, P., Fowler, P., and Roehrig,
    J. R.: A Cold-Cathode Ion Source Mass Spectrometer
    Employing Ion Counting Techniques. NASA CR-1475, 1969.

3. Torney, F. L., Jr., and Roehrig, J. R.: Research and
    Development Program on the Use of Counting Techniques.
    NASA CR-1747, 1971.

4. Blum, P., and Torney, F. L.: Cold-Cathode Quadrupole
    Mass Spectrometer. Rev. Sci. Instr., Vol. 38, No. 10,
    Oct. 1967, pp. 1404-1408.

5. Roehrig, J. R.: Program to Produce a Flight Prototype
    Cold-Cathode Quadrupole Mass Spectrometer. NASA CR-66793,
    1968.

6. Arnold, W.: Influence of Segmented Rods and Their
    Alignment on the Performance of a Quadrupole Mass
    Filter. Jour. Vac. Sci. and Tech. Vol. 7, No. 2,
    No. 1, Jan/Feb., 1970 pp. 191-194.

7. Woodward, C. E.; and Crawford, C. K.: Design of a
    Quadrupole Mass Spectrometer. Laboratory for In-
    sulation Research. MIT Technical Report 176, Jan. 1963.

8. Redhead, P. A., Hobson, J. P., and Kornelson, E. V.: The Physical Basis of Ultrahigh Vacuum. Chapman and Hall, Ltd. 1968.

62

APPENDIX A

CCIS OUTGASSING AND CONDUCTANCE CALCULATIONS

APPENDIX A

CCIS OUTGASSING AND CONDUCTANCE CALCULATIONS

A. **Outgassing and Conductance of CCIS/Quad**

The equilibrium partial pressure in the CCIS due to outgassing has been determined to be 1.35×10^{-12} Torr (H_2). Figure A1 illustrates the conductances of the CCIS/Quad which are used to determine the CCIS partial pressure. Table A1 lists the appropriate dimensions of orifices as illustrated in Figure A1.

TABLE A1

	Radius a(cm)	Length l(cm)	l/a	k	F_e (AIR) (liter/sec)	$F_t(H_2)$ (liter/sec)
O_1	0.28	0.5	1.8	0.538	1.54 x 8 holes	5.75 x 8 holes
O_2	0.095	0.076	0.8	0.72	0.238	0.89
O_3	0.75	9.0	12.0	0.172	3.55	13.3
O_4	0.0250	.025	0.1	0.96	2.2	8.22

where k is the Clausing correction factor, F_t (Air) = k x $36.66 \times 10^3 \, a^3$ (cm³/sec) or $36.66 \, a^2$ (liters/sec)

$$F_t \, (H_2) = \left[\frac{M(air)}{M(H_2)}\right]^{\frac{1}{2}} \times F_t \, (Air) = 3.74 \, F_t \, (Air)$$

Temperature assumed to be 25°C.

In calculating the partial pressure in the CCIS we assumed that $P_2 = P_4$ and also that the combined conductance of (C_o and C_1) = C_1, where C_1 consists of eight holes through cathode K_1 pole piece.
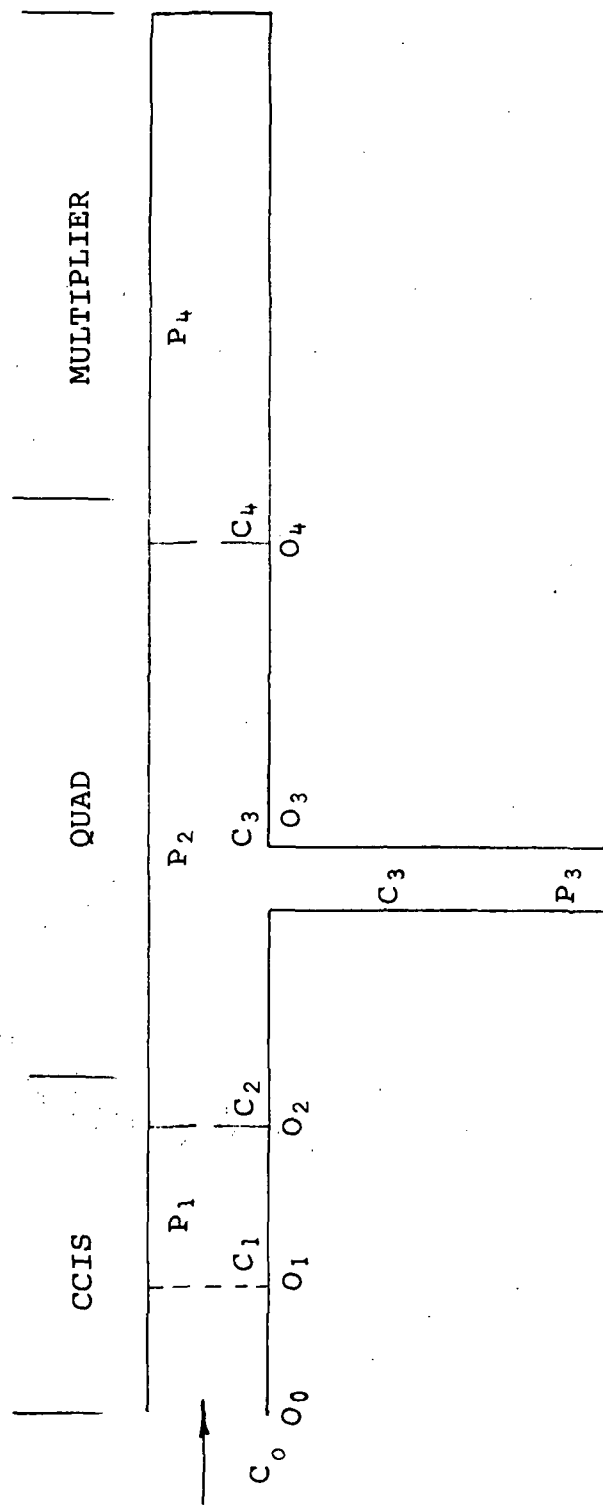
A-3

Figure Al. - CCIS Quad Conductance Diagram.

Total surface area contained within the Quadrupole analyzer and multiplier housing has been estimated to be $\approx$ 250 cm². This value includes rods, multiplier, deflection plates, etc.

Thus using Calder and Lewin[*] data for H_2 outgassing of stainless steel after 300°C bake for 25 hours.

$$\dot{Q}(H_2) = 4 \times 10^{-12} \text{ Torr-}\ell/\text{cm}^2 \text{ sec}$$

Therefore

$$Q \text{ (Total)}_{H_2} = 4 \times 10^{-12} \times 250 = 1 \times 10^{-9} \text{ Torr-}\ell/\text{sec } (H_2)$$

To determine P_2, the total conductance of $C_2 + C_3$ from Table A1 is 14.2 liter/sec (H_2). Therefore,

$$P_2 = \frac{Q_T}{C_T} = \frac{1 \times 10^{-9}}{14.2} = 7.0 \times 10^{-11} \text{ Torr } (H_2)$$

Since special outgassing procedures had been followed in the preparation of the CCIS, we here neglect the partial pressure contributions of CCIS outgassing.

Assumed $P_2 \gg P_1$, then throughput through orifice O_2 will be:

$$\dot{Q}_2 \approx P_2 \times F_{t_2} = 6.2 \times 10^{-11} \text{ Torr-Liter/sec}$$

---

[*]British Journal Appl. Physics 1967, Vol. 18, pp. 1468.

From Table Al the conductance of C_1.

$$C_1 = 5.75 \times 8 = 46 \text{ liter/sec} \quad (H_2).$$

Therefore CCIS partial pressure is seen to be:

$$Po = \frac{\dot{Q}_T}{C_T} = \frac{6.2 \times 10^{-11}}{46} \simeq 1.35 \times 10^{-12} \text{ Torr} \quad (H_2)$$

APPENDIX B

QUAD ELECTRONIC ADJUSTMENTS: THEORETICAL CONSIDERATIONS
OF THE "CONSTANT Δm MODE"

APPENDIX B

ELECTRONIC ADJUSTMENTS: THEORETICAL CONSIDERATIONS
OF THE "CONSTANT Δm MODE"

Early studies of the lunar mass spectrometer (ref. 1)
indicated reduced sensitivities to the higher mass portion
of the spectrum, especially for argon and xenon. It was
found that by making certain internal adjustments to the
commercial rf-dc generator electronics that the sensitivity
for these masses could be improved.

For the experiments reported herein, these adjustments
were again realigned to optimize high mass sensitivity con-
sistent with the resolution requirements noted in the state-
ment of work. Subsequent analysis of the experimental results
indicated that although the drive electronics were adjusted
to optimize resolution and sensitivity for higher masses,
sensitivity at the low end was decreased slightly thereby.
This fact is indicated by peak narrowing in the spectra of
Figures 7 and 8 for masses < 30 amu.

It can be shown that it is impractical to design a
quadrupole mass spectrometer for the 1-150 amu mass range,
within the power and sensitivity constraints of a lunar mission,
which also features 100% transmission for all ions. As a result
of practical power and sensitivity trade-offs, fractional trans-
mission will occur, at least over some portion of the mass range.
This condition normally leads to additional transmission loss
as a function of mass, especially for the highest masses.

It has been shown by Woodward and Crawford (ref. 7) that fractional transmission can be made nearly independent of mass. Briefly stated, the principal cause of fractional transmission is excessive transverse ion injection momentum. Woodward shows that the maximum transverse momentum for 100% transmission (and on axis injection) may be expressed as a voltage by the following equation:

$$U_{t_o} = \frac{V}{30} \frac{\Delta m}{M} \quad \text{(volts)} \tag{B1}$$

where U_{t_o} is the maximum transverse momentum, V is the peak rf voltage, M is the selected mass, and Δm the peak width (at the base). In this relation, V/M is a constant if the quadrupole is swept with variable rf voltage at a constant frequency, ν. Therefore if this maximum transverse momentum is not exceeded, Δm will be constant.

Woodward and Crawford also show that if the dc (U) and rf (V) voltages used to sweep the mass spectrum (at constant frequency) are related by a simple equation of the form

$$U = aV - b \quad \text{(a and b are constants}^*) \tag{B2}$$

that mass-dependent transmission (sensitivity) may be eliminated over a large portion of the spectrum. The constants "a" and "b"

---

*In the commercial quadrupole electronics, "a" is set by the external resolution control and "b" is set by an internal control.

are chosen from the following relation which is readily de-
rived from quadrupole theory:

$$\Delta m \simeq 7.94 \ (0.16784 - a) \ M + \frac{1.10b}{\nu^2 r_o{}^2} \ , \quad \text{(amu)} \qquad \text{(B3)}$$

If "a" is chosen to be exactly 0.16784, this equation shows
that the peak width Δm, will be independent of mass.[†] There-
fore, the maximum transverse injection momentum dictated by
eq.B1 will also be independent of mass. If then, this maximum
momentum is exceeded, trnasmission will be less than 100%,
but it will be <u>independent</u> of mass.

It should be noted that the constant "a" is simply the
ratio of the dc rod voltage to the peak rf rod voltage (U/V).
Measurement of this ratio to a sufficient accuracy is difficult.
The procedure to be described next is more straightforward.

The adjustments for "a" and "b" were made by first setting
b = 0. Then "a" was adjusted to "pinch off" all mass peaks;
that is, to approach infinite resolution. Next "b" was
adjusted to broaden all peak widths to approximately 1 amu.
In retrospect, it appears that "a" was initially adjusted to a
value slightly less than 0.16784. When "b" was subsequently
adjusted, all peak widths broadened, although the higher masses
broadened disproportionately, indicating that the mass de-
pendent term of equation 3 was not identically zero. Since
the required resolution for argon has been achieved, further
adjustments were discontinued.

---

[*]Equation 3 is approximately correct for $M/\Delta m > 5$. This
equation defines the so called "constant Δm mode". The same
basic equation is cited by Arnold (ref. 6) but the effect on
mass dependent transmission has not been discussed.

For the medium range the initial value of "a" was made more nearly equal to 0.16784 and adjusting "b" resulted in a more nearly constant Δm mode of operation.

Subsequent to the in-house tests, the adjusted value of "b" for the low range was determined to be equal to 0.19 volts. Substituting this value of "b" into equation (B3), together with a measured value of Δm ≃ 1 amu at mass 40 (from Figure 8), the actual value of "a" is calculated to be 0.1653. This value for "a" is next substituted back into equation (B3), to obtain an expression which shows how Δm actually varies with mass. This new expression may be simplified as follows:

$$\Delta m \simeq 2.162 \times 10^{-2} M + 0.1553 \text{ (amu)} \tag{B4}$$

Table B1 lists four values of Δm calculated from equation (B4) and compares these with observed values obtained from Figure 8 data. In general, the agreement is reasonably good.

Mass	Δm Calculated (eq.B4)	Δm Observed Fig. 8 @ 10% PK
12	0.41 amu	.4 amu
20	0.59 amu	.5 amu
28	0.76 amu	.7 amu
40	1.00 amu	1.0 amu

Finally, additional adjustments were made to the rf-dc generator electronics to improve the symmetry of both the dc and rf peak potentials with respect to ground. The latter adjustment was made by varying a differential capacitor connected to the two outputs and ground. Varying this capacitor balances the capacitive load as seen from each end of the rf output transformer. The effect of these adjustments was to improve peak shape when operating with long cables.

B-7

APPENDIX C

POWER AND WEIGHT ESTIMATES FOR FLIGHT TYPE CCIS/QUAD

APPENDIX C

POWER AND WEIGHT ESTIMATES FOR FLIGHT TYPE CCIS/QUAD

The Contract Statement of Work requires that estimates be prepared for the power, weight, and size of a flight configured design of the CCIS/Quad mass spectrometer. Without the information normally obtained by the design, construction and test of a prototype model, estimates of size and weight are generally somewhat speculative. Power estimates are likely to be more accurate because they are derived from physically measureable parameters. These estimates will be made first.

Power Estimates. - In a previous NASA development (ref. 5), a small, lightweight, low power CCIS/Quad mass spectrometer was designed, built and tested. This instrument included not only the necessary quadrupole drive electronics, but all other electronics required to operate and read-out the mass spectra on a dc current basis. The present CCIS/Quad analyzer tube is basically the same quadrupole, operating with the same rf frequency and rod voltage, and measuring the same mass range (0-50 amu). Because the rods are hyperbolic, a small increase in capacitance has resulted[*]. From the familiar quadrupole power equation,

$$P = \frac{6.5 \times 10^{-4} \ CM^2 \ \nu^5 \ r_o^4}{Q} \ , \ \text{watts} \qquad (C1)$$

---

[*]28.5 pf for the hyperbolic rods, vs. 22.5 pf for the round rod version.

it can be seen that the only parameter differing from the previous design is capacitance, C. This will result in a power increase of 28.5/22.5 = 1.27 times the ref. 5 design, and will effect only the quadrupole power budget. The net result will be to increase overall power slightly. The original design required an average power of 5.25 watts from 28 volts. Of this total. 4.0 watts was attributable to the quadrupole circuitry, including a dc-to-dc converter. With the slight increase in power due to capacitance differences, this portion increases to 1.27 x 4.0 = 5.1 watts. The total power on the 0-50 amu range will therefore be

Quadrupole Electronics	=	5.10 watts
H. V. Supplies & Log Electrom.	=	<u>1.25 watts</u>
TOTAL	=	6.35 watts

We round off this figure to 6.5 watts average power for the 0-50 amu range.

On the 45 to 150 amu range, the frequency factor, ν^5 has been <u>decreased</u> by $(3.98/6.0)^5 = 0.1281$, while the mass factor M^2 has increased by $\left(\dfrac{150}{50}\right)^2 = 9.00$. The overall power increase is therefore, 0.1281 x 9.00 = 1.15, if the instrument is swept from 0-150 amu. In sweeping from 45 to 150 amu, the average power is increased slightly. It can be shown that in scanning from 45 to 150 amu at 3.98 mHz, the average quadrupole power is 6.6 watts. The total instrument power on the 45 to 150 amu range would be:

C-4

```
Quadrupole Electronics               =  6.6 watts
H. V. Supplies & Log Electrometer  =  1.25 watts
                            TOTAL      7.85 watts
```

We round this figure off to 8.0 watts average power for
the 45-150 amu range.

The above discussions reference power to the 28 volt
supply and include certain efficiency factors which are in-
herent design variables. Improvement may be possible in
both the dc-to-dc converter and also in the "Q" of the
quadrupole tank circuit. Also the rf frequency actually
used during these tests is slightly higher than originally
planned. If the medium range frequency was reduced to
3.865 mHz instead of 3.98 mHz the frequency factor, ν^5,
would exactly cancel the mass factor, M^2, so that $\nu^5 \times M^2 =$
1.000. This would reduce the average power on the medium
range so that it would be about 7.0 watts. The effect on
resolution would be negligible.

In summary, it has been shown that the average power re-
quirements of the CCIS Quad are indeed modest. Using actual
power measurements derived from a previous instrument, the
power budget can be predicted for the 45-150 amu range to be
about 7.0 watts. On the 0-50 amu range, the average power
would be about 6.5 watts.

Size and Weight Estimates. - Again referring to the
small CCIS/Quad cited in ref. 5, we estimate size and weight
as follows. The small CCIS/Quad weighed 4 lbs. 13 oz. complete.

Additional electronics must be provided to scan the 45-150 amu range. It is conservatively estimated that the necessary electronics and mounting hardware would add approximately 1 3/4 lbs. Then the total weight would be about 6½ lbs.

Obviously, additional weight must be reserved for other hardware necessary to perform an actual experiment, such as breakseals, thermal control mechanisms, tape reels and support legs. It is estimated that this accessory hardware would bring the total weight to approximately ten pounds.

With regard to size, it is estimated that a flight experiment package could easily be housed in a rectilinear container whose dimensions are 6 x 6 x 14 inches overall (stowed configuration). These estimates are based in part on the previous CCIS/Quad of ref. 5, which was 4½ inches in diameter by 13 inches long, overall.